INITIAL ISEE MAGNETOMETER RESULTS: MAGNETOPAUSE OBSERVATIONS

C. T. RUSSELL and R. C. ELPHIC

Institute of Geophysics and Planetary Physics, University of California, Los Angeles, Calif. 90024, U.S.A.

Abstract. The magnetic field profiles across the magnetopause obtained by the ISEE-1 and -2 spacecraft separated by only a few hundred kilometers are examined for four passes. During one of these passes the magnetosheath field was northward, during one it was slightly southward, and in two it was strongly southward. The velocity of the magnetopause is found to be highly irregular ranging from 4 to over 40 km s^{-1} and varying in less time than it takes for a spacecraft to cross the boundary. Thicknesses ranged from 500 to over 1000 km.

Clear evidence for reconnection is found in the data when the magnetosheath field is southward. However, this evidence is not in the form of classic rotational discontinuity signatures. Rather, it is in the form of flux transfer events, in which reconnection starts and stops in a matter of minutes or less, resulting in the ripping off of flux tubes from the magnetosphere. Evidence for flux transfer events can be found both in the magnetosheath and the outer magnetosphere due to their alteration of the boundary normal. In particular, their presence at the time of magnetopause crossings invalidates the usual 2-dimensional analysis of magnetopause structure. Not only are these flux transfer events probably the dominant means of reconnection on the magnetopause, but they may also serve as an important source of magnetopause oscillations, and hence of pulsations in the outer magnetosphere. On two days the flux transfer rate was estimated to be of the order of 2×10^{12} Maxwells per second by the flux transfer events detected at ISEE. Events not detectable at ISEE and continued reconnection after passage of an FTE past ISEE could have resulted in an even greater reconnection rate at these times.

1. Introduction

The magnetopause has now been studied with in-situ spacecraft measurements for over a decade and a half. Much work has been performed on the average position and shape of the magnetopause (Cahill and Amazeen, 1963; Frank and Van Allen, 1964; Freeman, 1964; Ness *et al.*, 1964; Bridge *et al.*, 1965; Holzer *et al.*, 1966; Wolfe *et al.*, 1966; Cahill and Patel, 1967; Heppner *et al.*, 1967; Ness *et al.*, 1967; Binsack, 1968; Fairfield, 1971). As a result we now know the average position and shape of the forward position of the magnetopause quite well. The magnetopause position also varies with geomagnetic activity (Holzer *et al.*, 1966; Patel and Dessler, 1966; Cahill and Patel, 1967; Gosling *et al.*, 1967; Heppner *et al.*, 1967; Feldstein, 1970; Meng, 1970). It is now known that the cause of such variation is not simply variations in the external (solar wind) and internal (ring current) plasma pressure but also due to the erosion of the dayside magnetospheric flux under the influence of a southward directed interplanetary, and hence magnetosheath magnetic field (Aubry *et al.*, 1970, 1971; Russell *et al.*, 1974; Holzer and Slavin, 1978).

The magnetopause is constantly in motion with velocities greater than that of the spacecraft. This velocity is often periodic leading to multiple crossings. These multiple crossings and, in a few cases, energetic particle shadowing have been

Space Science Reviews **22** (1978) 681–715.

used to deduce velocities along the boundary normal of up to many tens of kilometers per second (Holzer *et al.*, 1966; Heppner *et al.*, 1967; Cummings and Coleman, 1968; Kaufmann and Konradi, 1969, 1973; Aubry *et al.*, 1970, 1971; Ledley, 1971). The structure or magnetic signature of the boundary has also been studied revealing a bewildering variety of signatures (Sonnerup and Cahill, 1967, 1968; Sonnerup, 1971; Aubry *et al.*, 1971; Ogilvie *et al.*, 1971; Sonnerup and Ledley, 1974; Neugebauer *et al.*, 1974). Comparison of these structures with theory has been difficult, although occasional 'classic' signatures are found (Sonnerup and Ledley, 1978). This difficulty is due in part to the complexity of the signatures, in part to the unknown relative velocity and in part to the variability of the orientation of the boundary in the course of a boundary crossing.

The ISEE mission has as one of its prime objectives the unfolding of the mystery of the structure of the magnetopause. To this end it includes high time resolution measurements of the magnetic and electric fields, low energy plasma and energetic particles. Furthermore many of the plasma and particle measurements are three-dimensional so that flows and anisotropies are not missed, nor misidentified. In addition many of the measurements are duplicated, or nearly so on both the closely spaced spacecraft. Thus time of flight measurements can be used to determine boundary velocities and hence thickness for quantitative comparisons with theory, and successive profiles can be compared to determine the time-stationarity of the boundary.

Recently two important papers on reconnection at the magnetopause have appeared. The first by Haerendel *et al.* (1978) proposes on the basis of HEOS-2 magnetic field and plasma data that reconnection occurs at the polar cusps and is impulsive. The second by Mozer *et al.* (1978) proposes on the basis of ISEE-1 magnetic and electric field data that at least one example of quasi-steady state reconnection has been found. In this paper we examine only four magnetopause crossings, and although we attempt to analyze these exhaustively, we cannot claim to have made a sufficient survey to say where reconnection takes place or to say if situations such as discovered by Mozer *et al.* (1978) are common or rare. In fact at this writing, we cannot even subject the set of crossings discussed by Mozer *et al.* to the analysis given in this paper because the requisite ISEE-2 data have not been received. Nevertheless, as will become evident in the sections to follow, we can show that reconnection does occur when the magnetosheath field is southward, very much in the impulsive manner envisioned by Haerendel *et al.* (1978). We cannot, however, pinpoint the location of initiation of the reconnection event from the limited amount of data examined so far.

2. Analysis and Display

Since we are attempting to present data from many different magnetopause crossings in this paper we have adopted certain conventions for presenting the

data which will remain the same for all intervals and simplify intercomparisions. Before proceeding to examine the magnetopause crossings we wish to discuss these conventions.

In our data analysis we use three separate temporal resolutions: low resolution, 64-s averages; medium resolution, 12-s averages; and the full resolution of the instrument which ranges from $\frac{1}{4}$ to $\frac{1}{32}$ of a second per sample. The 64-s data is generally used for surveying the data, and calculating average field strengths and directions, e.g., when characterizing a crossing. The 12-s averages are overlapped by two thirds and calculated every 4 s. These averages are used to restrict the bandwidth of the analysis and reduce the number of data points, for example, when high frequency oscillations may obscure the gross structure of a boundary. Finally the full resolution of the instrument is used, whenever necessary, to define accurately the rapid variations often encountered at magnetospheric boundaries. These samples are averaged internal to the instrument and overlapped to avoid aliasing problems. A fuller description of the instrument can be found in Russell (1978) and in Russell and Greenstadt (1979).

For each of the crossings we will use a boundary normal coordinate system to display the medium resolution data (12-s overlapped averaged) across the entire interval of interest. The boundary normal system has its N-direction outwards along the boundary normal, its L-direction along the projection of the solar magnetospheric Z-direction perpendicular to the normal. The M-direction completes the right-hand orthogonal set. The purpose of choosing a local coordinate system rather than a global one is to reduce the variations in the data to two dimensions and thus make them easier to understand. We shall avoid the often confusing practice of displaying data in terms of field magnitude and angles. We feel that the common practice of displaying field directions in terms of ecliptic longitude and latitude has previously obscured certain obvious features, examples of which are conspicuous in data we will be discussing.

We use three techniques to determine normals. If the boundary is a tangential discontinuity, then there is no field along the boundary normal and the vector cross product of the fields on either side of the boundary gives the direction of the normal. Second, if the boundary contains a clear rotation of the field which is relatively noise free and the normal does not appear to rotate during the crossing, a minimum variance technique (Sonnerup and Cahill, 1967) can be used. As we shall see, for the crossings discussed herein, this technique is often far from satisfactory. Thirdly, we can compute the normal from a model. The magnetopause model we use is a conic section with eccentricity 0.4 with focus at the Earth. The normal we use will depend on the particular circumstances of the crossing and will be explicitly stated.

For selected intervals we will also display the full resolution data and do principal axis or minimum variance analysis. The results of this analysis will be displayed in an **ijk** coordinate system with **i** along the eigenvector associated with the maximum eigenvalue and **k** along the direction of minimum variance. The

j-direction completes the right-handed set. These data will be displayed as hodograms of the tip of the field vector in the i-j and i-k planes.

Tables giving the location of the satellites, their separation, field directions normals, etc., will use solar magnetospheric (GSM) coordinates throughout. The GSM system has its X-direction pointing toward the Sun, its Y-direction perpendicular to the Earth's dipole and the Sun direction towards dusk and its Z-axis in the Sun-dipole plane northward.

The magnetometer zero levels are checked periodically by flipping the spin axis aligned sensor into the spin plane. Spacecraft associated fields were determined during a period of crossed spin axis operation by intercomparing data in the spin plane of one spacecraft with that along the spin axis of the other. Other than this one cross-check the data processing of both spacecraft has been completely independent. No adjustments have been made to either the phase in the spin plane, the offsets or the gain of the instruments to bring the data into alignment. When the satellites enter regions of essentially homogeneous fields, as we will see, the data from the two spacecraft coincide to within the resolution of the plots. All differences between spacecraft visible on these plots are due to real differences in the ambient field. None are due to spacecraft or instrument related sources.

3. Northward Magnetosheath Field, Orbit 6 In

One expects the least stable magnetopause to arise when the magnetosheath and magnetospheric magnetic fields are antiparallel; conversely, the most stable configuration should be obtained when the fields are parallel. Thus, we choose to begin our examination of the ISEE magnetopause data with what should be a comparatively simple crossing, in which magnetosheath and magnetospheric field directions differ by less than 25 deg. During this interval the ISEE spacecraft were at a solar magnetospheric position of (10.35, −1.13, 5.17) R_e with a separation of (259, −174, 215) km or 360 km along the model normal.

3.1. The macrostructure of the boundary

Figure 1 shows medium resolution, 12 s averages, of ISEE-1 and -2 measurements across the magnetopause from 16:48 to 17:24 on November 5, 1977. ISEE-1 data are plotted with a heavy line, ISEE-2 with a light line. The coordinate system is the boundary normal system with the normal chosen to be that of a tangential discontinuity. Table I lists many of the parameters relevant to this crossing including the direction of the model normal and the tangential discontinuity (TD) normal. We note that these two normals differ by over 14°, whereas when the field is southward as we will see in later sections the normals agree much more closely.

There are three distinct magnetic field regimes in Figure 1 which can be characterized by the behavior of the field magnitude. First, the period before 16:59 is typified by oscillating field strength which maximizes at 40γ. These

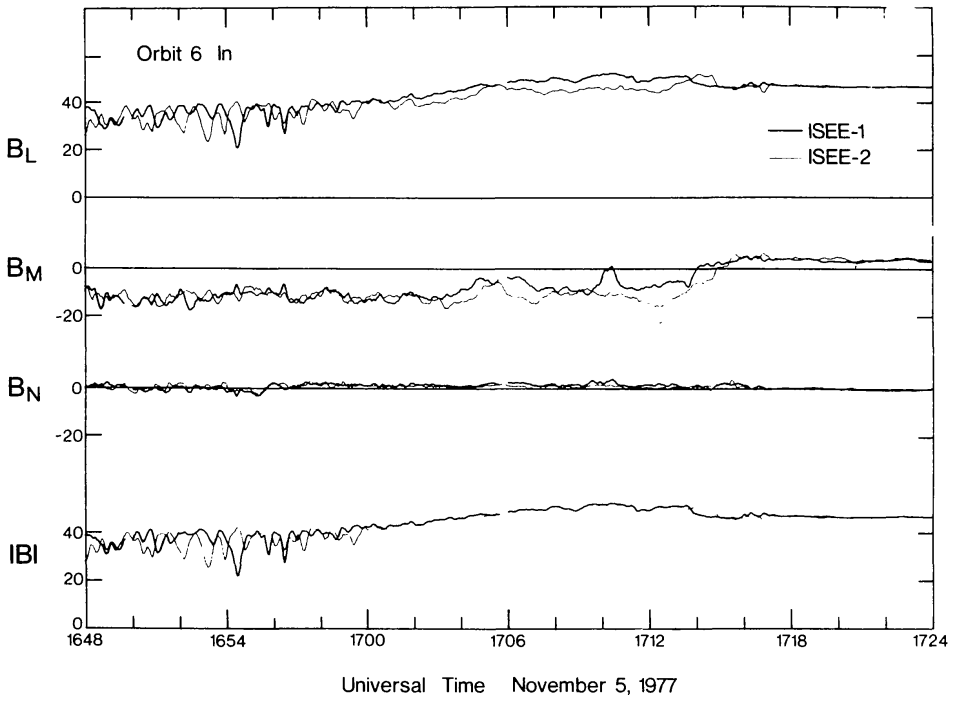

Fig. 1. Magnetic field measured by ISEE-1 (heavy line) and ISEE-2 (light line) across magnetopause on orbit 6 inbound, November 5, 1977. The coordinate system is oriented so that B_N is along the normal of the boundary assuming the boundary is a tangential discontinuity. B_L is along the projection of the solar magnetospheric Z-direction perpendicular to the boundary normal. The data shown here are 12 s averages calculated every 4 s, called medium resolution data. The scales on this and all following plots are in units of gammas ($1\gamma = 1$ nT). The ISEE spacecraft were at $(10.35, -1.13, 5.17)R_e$ in solar magnetospheric coordinates and separated by 360 km along the magnetopause normal.

oscillations in field strength show little coherence between the two spacecraft, even though the separation is only 380 km. We note that the transverse oscillations in B_N and to a lesser extent in B_M show high coherence. After 16:59 the oscillations decrease, and the magnitude rises to a peak of about 62γ before dropping suddenly at 17:14 on ISEE-1, followed by ISEE-2 roughly a minute later. Thereafter the field strength remains steady at about 47γ.

TABLE I
Magnetopause parameters

Time	Nov. 5, 1977 17:15 UT	Nov. 3, 1977 07:46 UT
Orbit	6 inbound	5 inbound
Location $\mathbf{R}_{GSM}$ (R_e)	(10.35, −1.13, 5.17)	(10.53, 0.46, 5.20)
Separation $\mathbf{S}_{GSM}$ (km)	(259, −174, 215)	(261, −106, 236)
$\mathbf{B}^{sh}_{GSM}(\gamma)$	(−13.8, 15.7, 28.1)	(2.0, 13.4, −4.5)
$\mathbf{B}^{ms}_{GSM}(\gamma)$	(−24.3, 1.6, 39.9)	(−15.4, −0.1, 42.3)
$\measuredangle \mathbf{B}^{sh}, \mathbf{B}^{ms}$	24.8°	110.3°
${}^{m}\mathbf{n}_{GSM}$	(0.943, −0.072, 0.325)	(0.946, 0.031, 0.322)*
${}^{TD}\mathbf{n}_{GSM}$	(0.835, −0.190, 0.516)*	(0.939, −0.025, 0.342)
$\measuredangle {}^{m}\mathbf{n}, {}^{TD}\mathbf{n}$	14.4°	3.9°
$\mathbf{S} \cdot \mathbf{n}$ (km)	360	320

* Normal used in calculations and plots.

The region before 16:59 UT is clearly the magnetosheath. The LASL/MPI fast plasma instrument shows that the plasma in this region is flowing with a velocity of from 80 to 100 km s^{-1} with a density of about 25 cm^{-3}. An interesting feature is that the plasma thermal pressure is anti-correlated with the field pressure here. Thus, the dips in the field strength appear as spikes in the plasma pressure (G. Paschmann, personal communication, 1978).

It is tempting to call the entire region from 16:59 to 17:14, the magnetopause. The two satellites have obviously entered a field structure, for ISEE-1 and -2 fields begin to differ significantly at this point, with ISEE-2 lagging ISEE-1 in field strength and direction. The time lag and the difference in field values are a complicated function of time and it is difficult to trace the motion of the boundary over the spacecraft until about 17:13 when the field changes at the two spacecraft are both unidirectional.

The variations in the plasma parameters during this crossing are initially as subtle as the field data (see Paschmann *et al.*, 1978). At about 16:59 the density slowly begins to decrease as does the plasma thermal pressure. At 17:12 on ISEE-1 and 17:13 on ISEE-2, the density drops more quickly. At about 17:14 on ISEE-1 and 17:15 on ISEE-2 the first proton temperature rise occurs followed by a second rise at 17:16 and 17:17 on the two spacecraft. This latter behavior is characteristic of the magnetopause boundary layer (Haerendel *et al.*, 1978). Thus the boundary layer straddles our final magnetopause current layer.

3.2. The microstructure of the boundary

Figure 2 shows the full resolution of the instrument in spacecraft coordinates for the ISEE-1 crossing of the main current layer. The bandwidth of the data here is 24 times that of Figure 1. We see an additional change upon crossing into the magnetosphere, namely the high frequency wave amplitude drops. The start of the boundary layer, BL, has been chosen to be the time of the onset of the rise in proton temperature as measured by the LASL/MPI fast plasma analyzer and the end to be the time of the last temperature rise accompanied by a density drop. Internal to the boundary layer a reversed flow was seen, directed towards the Sun with a velocity of greater than 60 km s^{-1}. There is no obvious signature of this flow in the magnetic field.

The correlation with the Berkeley/Toulouse energetic particles is also quite interesting. Enhanced fluxes of 2 keV electrons are first seen on ISEE-1 at 17:12:20 and on ISEE-2 at 17:13:55, roughly at the same location within the boundary crossing as judged by the phase of the field variation. Although the initial electrons were seen on ISEE-1 at 17:12:20, the final and strongest increase in electrons occurred at 17:13:30 coincident with the entry into the boundary layer as defined by the fast plasma instrument. The ISEE-2 data shows only a single electron increase and it is also coincident with the boundary layer defined by the fast plasma instrument. Enhanced fluxes of 2 keV protons are not

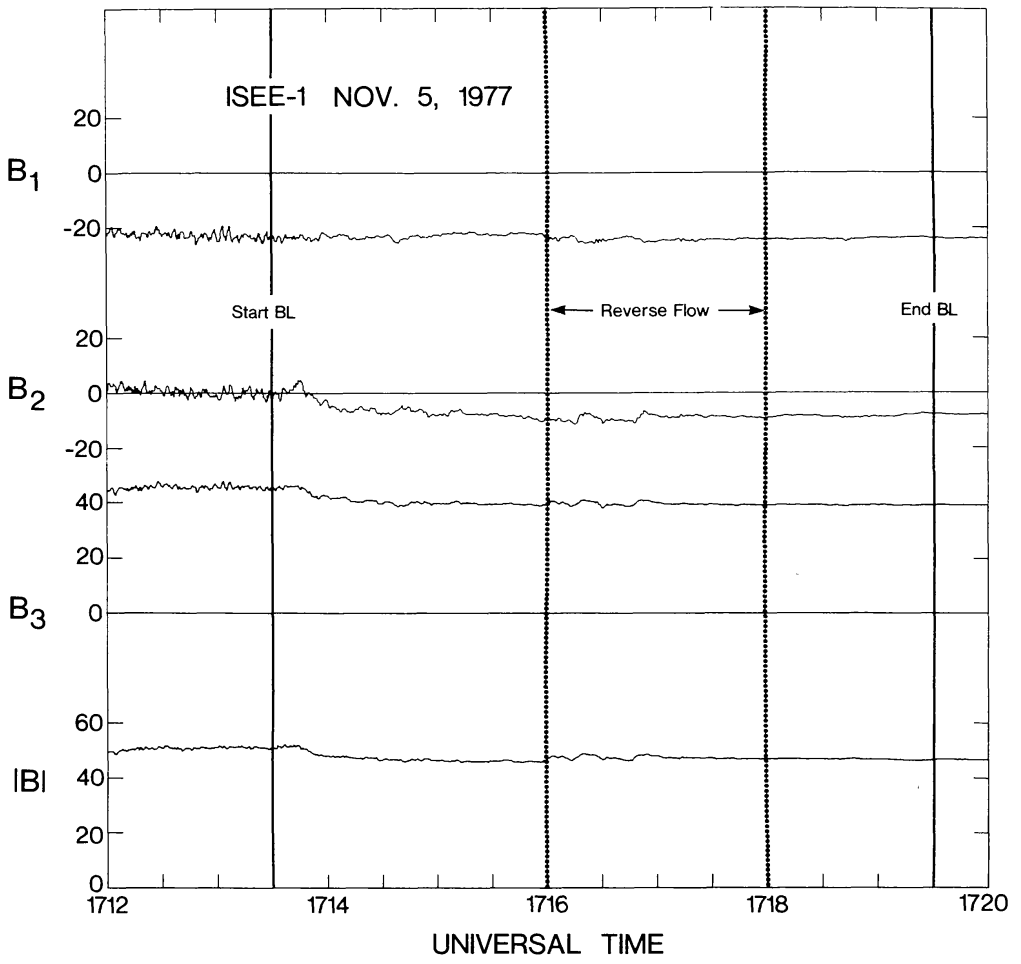

Fig. 2. High resolution ISEE-1 measurements (4 samples every second) through the magnetopause on November 5, 1977. Measurements are in spacecraft coordinates.

seen until somewhat later 17:13:45 on ISEE-1 and 17:14:40 on ISEE-2, essentially when ISEE had completely traversed the final current layer.

Figure 3 shows hodograms of the variation of the field through the magnetopause in boundary normal components. The $B_L - B_M$ plane is the plane of the boundary. We see roughly the same general variation on both ISEE-1 and -2. Initially on the magnetosheath side of the boundary there were strong fluctuations. Eventually the field rotates through about 30° and the fluctuations settle down to much lower magnetospheric levels.

3.3. Velocity and Thickness of the Magnetopause

If the magnetopause were stationary during this crossing, it would have a thickness of 2200 km, the distance travelled by the spacecraft along the normal from 16:59 to 17:15. However, the data suggest that the magnetopause is moving, sometimes irregularly during this crossing. In order to measure a velocity we have to find the same point on the boundary measured at different times by the two spacecraft. The only location in the magnetopause traversal discussed

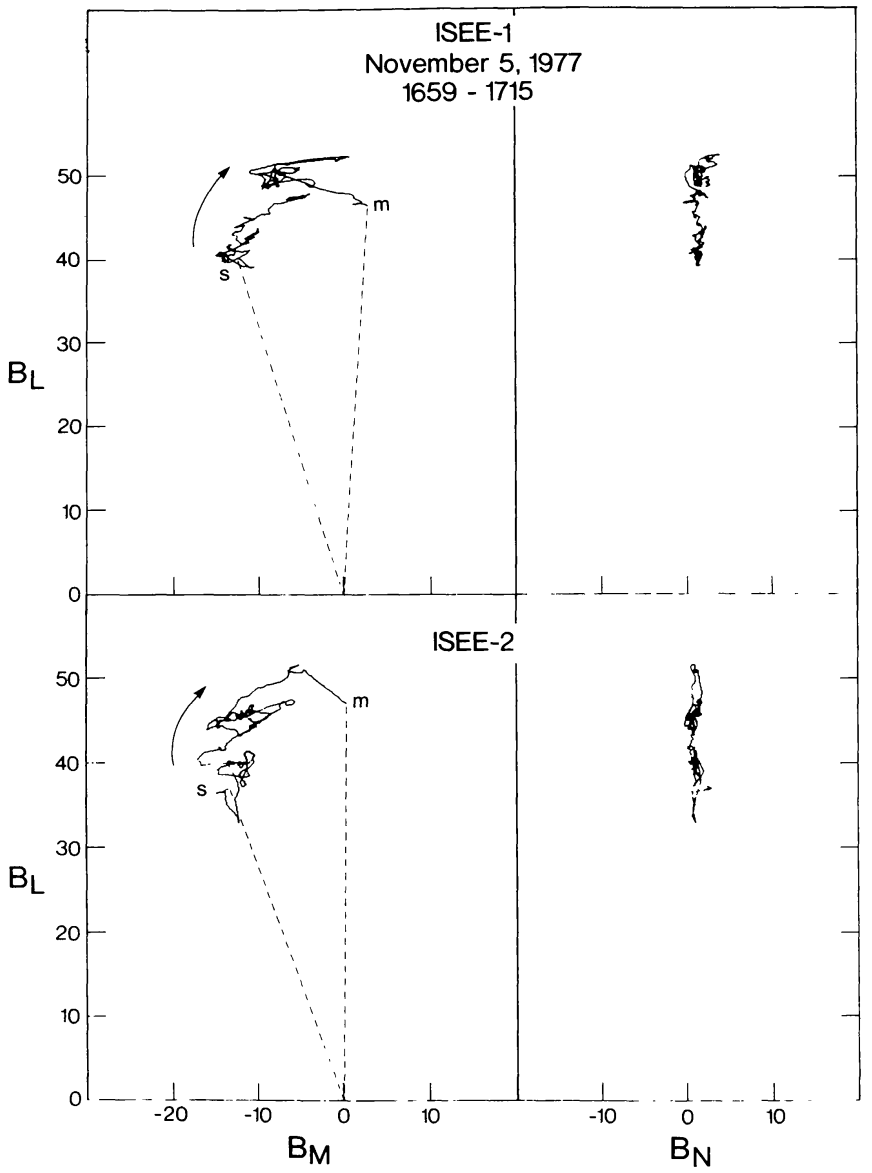

Fig. 3. Hodogram of the variation of tip of the magnetic field vector through the magnetopause on November 5, 1977. The data are 12 s averages rotated into boundary normal coordinates.

here for which this is unambiguously possible, assuming invariant structure, is in the crossing of the final current sheet at about 17:14.

Figure 4 shows the B_M component of the field for ISEE-1 and -2 from 17:13-17:18. At the line labelled '*a*' ISEE-1 and -2 are 360 km apart along the magnetopause normal. In 20 s, ISEE-2 reaches the same field value. Interpreting this as motion of the magnetopause relative to the two spacecraft, the resultant velocity is 18 km s^{-1}.

At this time, as indicated by the line labelled '*b*', ISEE-1, which is 360 km closer to the Earth, measures a new field value. ISEE-2 reaches this value 14 s later for an average velocity of 26 km s^{-1}. However, ISEE-1 has now moved further along the boundary to a new field value at '*c*', which ISEE-2 reaches 8 s later at an average velocity of 45 km s^{-1}.

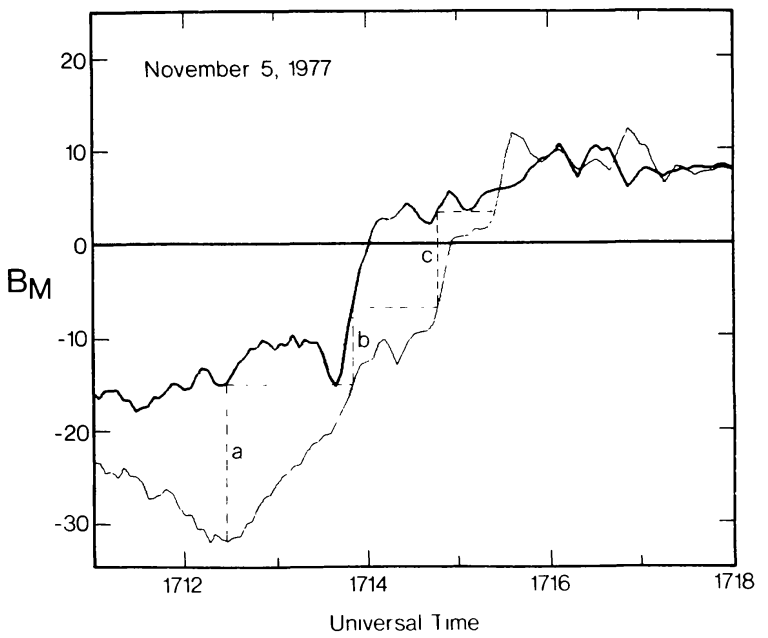

Fig. 4. Medium resolution averages of the B_M component of the field measured on ISEE-1 (heavy line) and ISEE-2 (light line) on November 5, 1977. At the time of the vertical lines labelled '*a*', '*b*', and '*c*', the two spacecraft were separated by 360 km along the magnetopause normal. Thus the current layer causing the B_M variation is over 1180 km thick.

Since it took three steps for us to traverse the boundary the current layer must have been about 1000 km thick. The velocity is quite irregular, varying from 18 to 45 km s^{-1} according to our calculations. However, if the gradients in the field are a measure of velocity, the instantaneous velocity must at times be even greater since we averaged over varying slopes.

3.4. Discussion

In a situation with a strong northward magnetic field, as we have here, we would expect that the magnetopause would be relatively simple. Perhaps it is, in comparison with the crossings we will be examining below. Nevertheless it has its complications. First, the velocity is quite variable and temporal variations in the structure confuse the determination of velocity and therefore thickness. Perhaps surprisingly, the magnetic field strength within the boundary is larger than the field in the magnetosheath or in the magnetosphere. This effect cannot be dismissed as due to a temporal change in external conditions during the crossing. Both ISEE-1 and -2 see the effect at different times as they pass through the boundary. Finally, again perhaps surprisingly, there is a boundary layer of plasma in the magnetosphere adjacent to the magnetopause, and even in the apparent absence of any reconnection between the magnetosphere and magnetosheath reverse flow of plasma to the Sun is seen in the boundary layer.

4. Horizontal Magnetosheath Field, Orbit 5 In

When thinking of the typical magnetopause, one usually considers the case in which the interplanetary and magnetosheath fields are in the ecliptic or equatorial plane and therefore at right angles to the magnetospheric field. The magnetopause crossing inbound on orbit 5 around 07:50 UT, November 3, 1977 occurred under nearly such conditions. The location of the ISEE spacecraft was (10.53, 0.46, 5.20) R_e in solar magnetospheric coordinates and their separation vector was (261, −106, 236) km. ISEE-1 was the lead spacecraft. The magnetosheath field was about (2.0, 13.4, −4.5)γ and the field just inside the magnetosphere was (−15.4, −0.1, 42.3)γ. Thus the angle between the magnetosheath and magnetospheric fields was locally about 110°.

4.1. The Macrostructure of the Boundary

Figure 5 shows the medium resolution data from 07:34 to 08:10 UT. ISEE-1 data are plotted with a heavy line, ISEE-2 data with a light line. The coordinate system is the boundary normal system with the normal chosen to be that of the model normal. As shown in Table I, the angle between the model normal and the

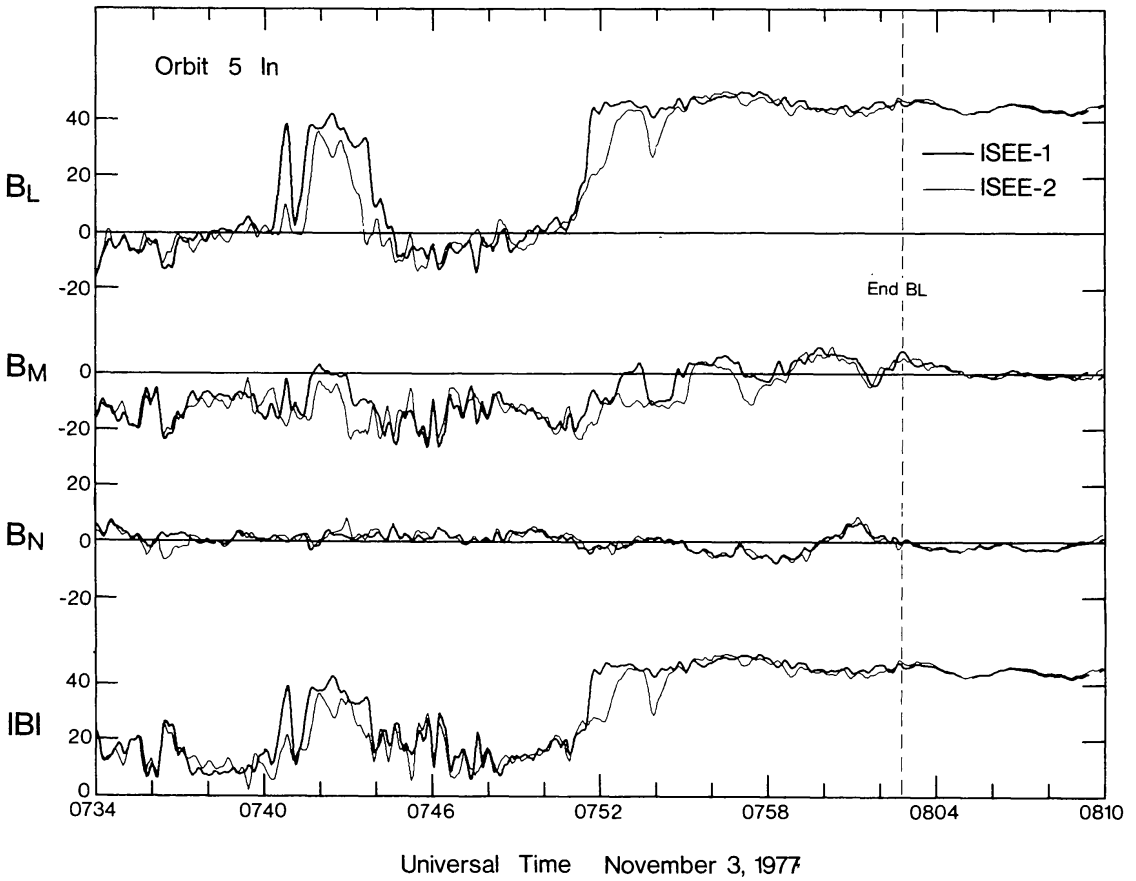

Fig. 5. The medium resolution magnetic field measured by ISEE-1 (heavy line) and ISEE-2 (light line) on November 3, 1977, expressed in boundary normal coordinates. ISEE-1 and -2 were at (10.53, 0.46, 5.20)R_e in solar magnetospheric coordinates and separated by 320 km along the normal at this time.

normal obtained from the assumption that the boundary is a tangential discontinuity is 3.9° deg, which is much closer agreement than the 14° obtained at a very similar position or orbit 6 inbound when the magnetosheath field was strongly northward.

As is most evident in the BL component and the total field there are 7 crossings or partial crossings seen by the two spacecraft, the first being at 07:41 and the last at 07:54. Since B_L is essentially along the Z-GSM direction, the field directions on the far right of this figure are those expected in the magnetosphere. We note how well the spacecraft fields track each other on the far right and far left of this figure; the deviations occur principally at the boundary crossings.

The field along the model normal, B_N, oscillates about zero and is everywhere less than 9γ in magnitude. The oscillations in this component again are highly coherent between the two spacecraft. This suggests that the source of the oscillations is the rocking back and forth of the true boundary normal. The oscillation of the B_N component of the field would be simply the local field magnitude times the sine of the angle between the model normal and the actual normal projected in the field-normal plane. Deviations of B_N of 1.5γ in the magnetosheath and 6γ in the magnetosphere correspond to fluctuations in the normal direction of about 7° but in nearly orthogonal directions.

The fluctuations in B_M are not as immediately interpretable. However the B_M trace does lead to some conclusions not readily evident in the other component. For example, since the B_M component does not reach magnetospheric levels during the 07:51-07:53 crossing on ISEE-2 we know the crossing was not complete. The fact that neither ISEE-1 nor -2 B_M components settle down to their final magnetospheric level until 08:05 suggests that something is occurring in this region that is not evident in the other components.

Perhaps the most useful component, however, is B_L. This component contains most of the field change across the boundary and hence is a good tracer of the distance travelled through the boundary. When ISEE-2 reaches a field value just previously attained by ISEE-1, we know the boundary relative to the satellite has moved along its normal a distance of 320 km, that is the separation distance between ISEE-1 and -2 measured along the model normal. Thus, the time delay between ISEE-1 and -2 can be converted to a velocity. We will defer discussion of the velocities derived from the behavior of B_L until later.

The boundary layer as determined by the LASL/MPI fast plasma instrument begins immediately inside the magnetopause and ceases at 08:03 UT. The field is somewhat more irregular in the boundary layer region than later in the magnetosphere. The variations in the B_M component suggest the presence of field aligned currents within the boundary layer.

4.2. The microstructure of the boundary

High resolution plots of the time series of the magnetic field data do not reveal appreciably different detail than is evident in the medium resolution plot shown in

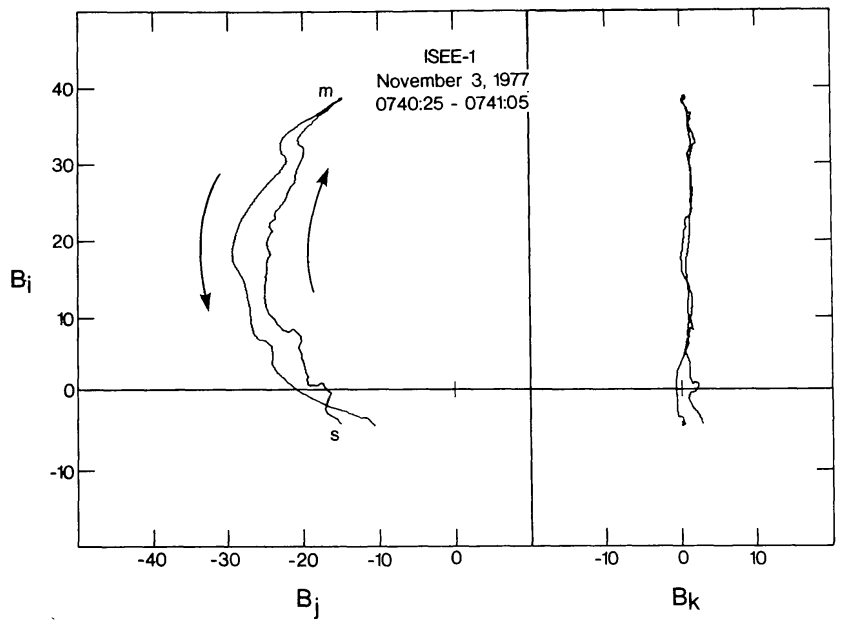

Fig. 6. Hodogram of the top of high resolution measurements of the magnetic field vector on ISEE-1 in the principal axis system for the first pair of in and out crossings on November 3 at 07:41.

Figure 5. Therefore we will next examine the hodograms of these boundary crossings. The first crossing of the magnetopause is centered about 07:40:30. There is almost a complete traversal by ISEE-1 and only a very partial crossing by ISEE-2. Minimum variance analysis of high resolution ISEE-1 data through this double crossing is shown in Figure 6. This pair of crossings is extremely close to the ideal compared to those that follow; first, the statistically determined minimum variance direction is only 3° different from the model normal, and second, the average field along the minimum variance eigenvector is not significantly different from zero, suggesting that this boundary is essentially a tangential discontinuity.

It is first apparent that ISEE-1 enters the boundary layer at 07:40:30, concurrent with the approximate midpoint of the first magnetopause crossing. While ISEE-2 makes a partial penetration of the magnetopause, no sign of the boundary layer is seen, and these two facts point out that the higher energy particles do not appear until part way into the main current sheet. A weak (<50 km s^{-1}) reversed flow was seen by the fast plasma analyzer at 07:40:50.

The third magnetopause crossing at 07:41:20 by ISEE-1 and 07:41:40 by ISEE-2 is accompanied by small variations in the B_N component, suggesting that the boundary normal direction is changing at this time. Since the principal axis directions were not sufficiently well determined to perform meaningful comparisons between ISEE-1 and -2, nor between adjacent crossings we have chosen simply to display the hodograms in boundary normal coordinates, using the high resolution data. These hodograms appear for ISEE-1 and -2 in Figure 7a; it is clear that differences between the two spacecraft traces reflect the variability of

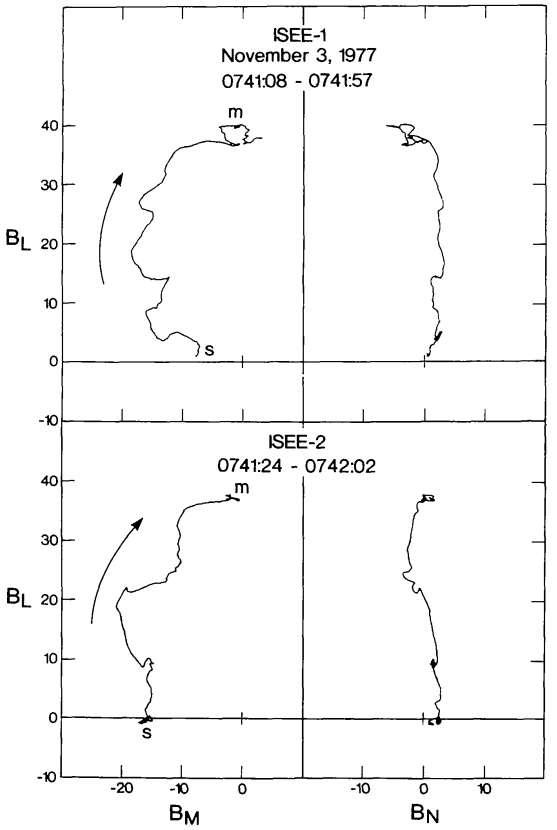

Fig. 7a. Hodogram of high resolution magnetic field data in boundary normal coordinates across 07:42 magnetopause.

the boundary orientation and structure. If, for example, differences in the B_N component in Figure 7a are due principally to changes in the boundary attitude, the maximum variation corresponds to changes in true normal direction of $\sim \pm 5°$. The differences in the ISEE-1 and -2 B_L vs B_M traces, while in broad agreement with Figure 6, point out the variability of the boundary micro-structure on temporal and spatial scales comparable to the crossing time and spacecraft separation distance.

At roughly 07:42:40 ISEE-2 begins the fourth magnetopause traversal, followed by ISEE-1 some 24 s later. This crossing is characterized by extreme departures from the relatively simple signatures of the initial crossings. High resolution hodograms in boundary normal coordinates are displayed in Figure 7b, in which are evident significant differences between the traces of the two spacecraft, as well as variations from the 'ideal' rotation. Most notably, a large drop in field magnitude occurs on ISEE-1 at the same point in the field rotation as a magnitude enhancement occurs on ISEE-2. Similar features appear more prominently in crossings analyzed in later sections of this paper, and discussion of these features is deferred until then. It is noteworthy that prior to this crossing at 07:42:30 on ISEE-2 and 07:42:40 on ISEE-1, results from the fast plasma analyzer indicate a change from boundary layer to a plasma with nearly magnetosheath densities, and flowing weakly reverse to the magnetosheath flow

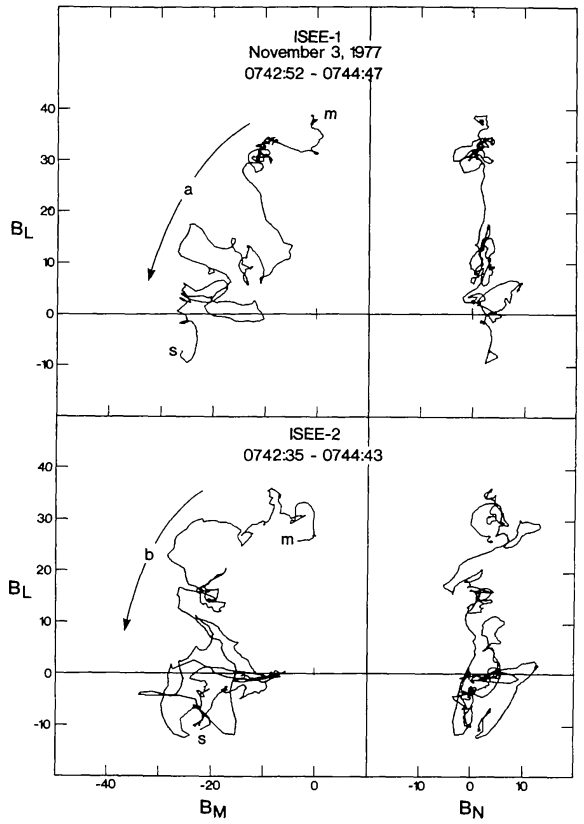

Fig. 7b. Hodogram of high resolution magnetic field data in boundary normal coordinates across 07:43 magnetopause.

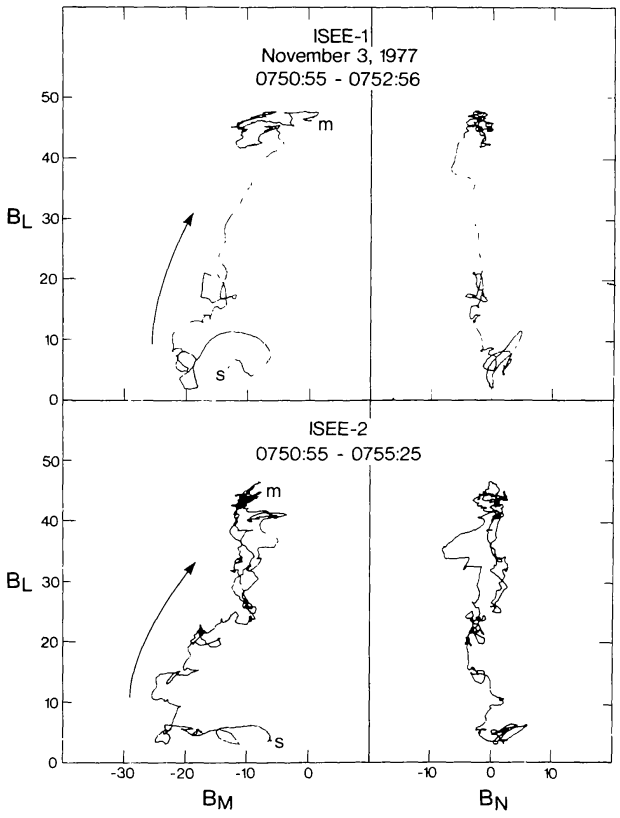

Fig. 7c. Hodograms of high resolution magnetic field data in boundary normal coordinates across 07:52 magnetopause.

direction. A true return to the magnetosheath as evidenced by the field and plasma experiments does not take place until 07:44.

The fifth and final full magnetopause crossing occurred at roughly 07:52 on ISEE-1 and 07:53 on ISEE-2. The boundary traversal is accompanied by entry into the boundary layer, which is seen as a strong reversed flow ($\sim 100\,\mathrm{km\,s^{-1}}$) on ISEE-1, and somewhat weaker ($\sim 50\,\mathrm{km\,s^{-1}}$) on ISEE-2, according to the LASL/MPI fast plasma analyzer. This reverse flow is seen on ISEE-1 until 07:52:30 when the bulk velocity direction begins to swing through anti-sunward flow to final downward flow at roughly 07:52:50. During this flow direction variation the B_M component on ISEE-1 changes from $\sim -10\gamma$ to $\sim 0\gamma$. The signatures of the high resolution hodograms for this crossing, seen in Figure 7c, are yet another variant of the basic rotation seen on the earliest crossings. Not only is the rotation less circular, but the final magnetospheric field strength is greater than in previous crossings. Changes in the B_N component, if due to boundary attitude variations, lead to angular oscillations of roughly $\pm 5°$ or less. The flow direction change seen at 07:52:40 on ISEE-1 corresponds to the topmost rotation, in which B_M goes from $\sim -10\gamma$ to 0γ.

4.3. Velocity and thickness

To obtain boundary velocities relative to the spacecraft on this pass, we have determined the time delay required for the two spacecraft to consecutively attain the same position in the B_L field gradient. These time delays are shown as the horizontal lines in Figure 8, and have been (wherever possible) spaced uniformly in time, not in pseudo-distance through the boundary. The lines range from 7 to 71 s duration, and given the spacecraft separation along the normal (320 km), these times yield the relative boundary velocity plotted below the field trace. We note that these are average velocities over the time span denoted by the horizontal lines in the B_L trace; negative velocities indicate motion of the magnetopause towards the Earth, positive away. The 07:52 crossing is interesting in that an initial very rapid motion is present, followed by an almost exponential deceleration. The average boundary speed and its standard deviation from the 32 determinations here are $15.9 \pm 9.8\,\mathrm{km\,s^{-1}}$. The median speed was $15.1\,\mathrm{km\,s^{-1}}$.

Measuring the total thickness of the boundary is difficult for several reasons. First, the velocity is quite variable during these crossings. Second, no crossing from unambiguous magnetosheath to unambiguous magnetosphere seems to be made. Third, the relation between B_M field value and distance through the boundary is non-linear. Nevertheless, we can get an approximate value for the thickness of the boundary using the staircase approach of the previous section.

The first magnetopause traversals are partial crossings of the boundary, so only a fractional thickness may be obtained. ISEE-1, however, appears to achieve nearly the magnetospheric configuration, and a stepwise calculation of the entry and exit thicknesses of the magnetopause yield ~ 520 and ~ 640 km, respectively. For the third crossing, in which ISEE-1 appears to traverse the boundary

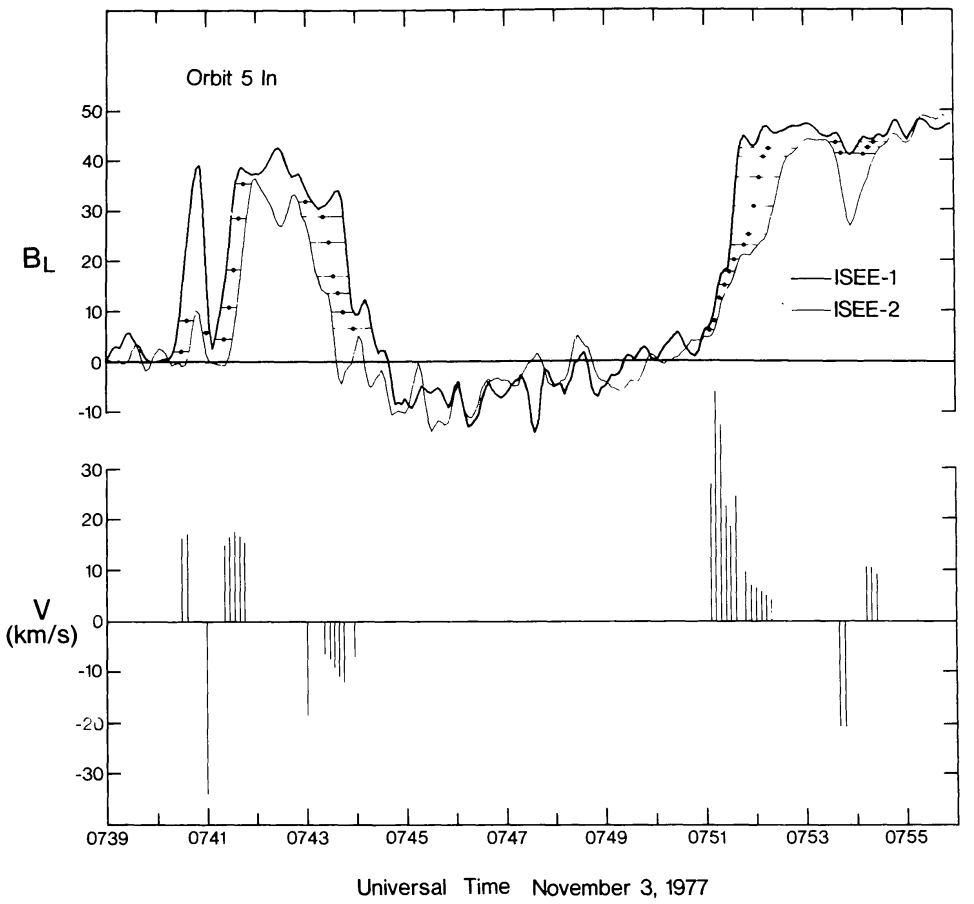

Fig. 8. Medium resolution averages of the B_L component of the ISEE-1 (heavy line) and ISEE-2 (light line) measurements through the magnetopause on November 3, 1977. The short horizontal line segments joining the ISEE-1 and ISEE-2 traces at common values of B_L provide measures of the time delay between ISEE-1 and -2. At the center time of each of these intervals we have calculated the average velocity over the time interval of the line segment, and have plotted these in the bottom panel of the figure. Velocity estimates are equi-spaced in time whenever single-valued velocities could be deduced.

completely, between two and three steps are required, giving a thickness of ~640 to ~960 km. In the fourth magnetopause encounter, boundary speed and structure variations complicate the thickness determination, but it seems clear that at least two and possibly three steps are needed to enter the magnetosheath, giving a thickness once again of approximately 640–960 km. The final full crossing likewise suffers from boundary structure and velocity changes, but appears to require at least three steps for the full crossing. Thus, this magnetopause is evidently the thickest traversed on this pass, being at least ~960 km thick.

5. Southward Magnetosheath Field, Orbits 7 In

The occurrence of geomagnetic storms and substorms is controlled by the southward component of the interplanetary magnetic field (Arnoldy, 1971; Russell and McPherron, 1973; Burton *et al.*, 1975). Further, the magnetopause

appears to be eroded when the interplanetary field is southward (Aubry *et al.*, 1971). Thus, we would expect that increasingly southward fields would lead to an increasingly stressed magnetopause. In the next two sections we will examine two such magnetopause crossings. The first crossing occurred on November 8, 1977 at about 02:50 UT. The ISEE spacecraft were at (10.16, −1.77, 5.07) R_e in solar magnetospheric coordinates and were separated by (231, −181, 192) km again in GSM. The separation along the model normal was 299 km. The angle between the average magnetosheath field and the magnetospheric field locally ranged from 115° to 145°.

5.1. The Macrostructure of the Boundary

Figure 9 shows the medium resolution data from 02:00-03:06 UT. The ISEE-1 data are plotted with a heavy line; the ISEE-2 data with a light line. The coordinate system is the boundary normal system using the model normal. As shown in Table II, the angle between the model normal and the tangential discontinuity normal is 0.6°, using the 02:02 sheath field and the 03:04 magnetospheric field and 2.5° using the 02:43 sheath field.

If one were to examine solely the B_L and $|B|$ traces, one would interpret this section of data to contain two partial entries into the magnetosphere: one at 02:12 and one at 02:36 together with a full entry, albeit with much back and forth motion, from 02:44 to 02:52. The B_L traces are nested as expected for an

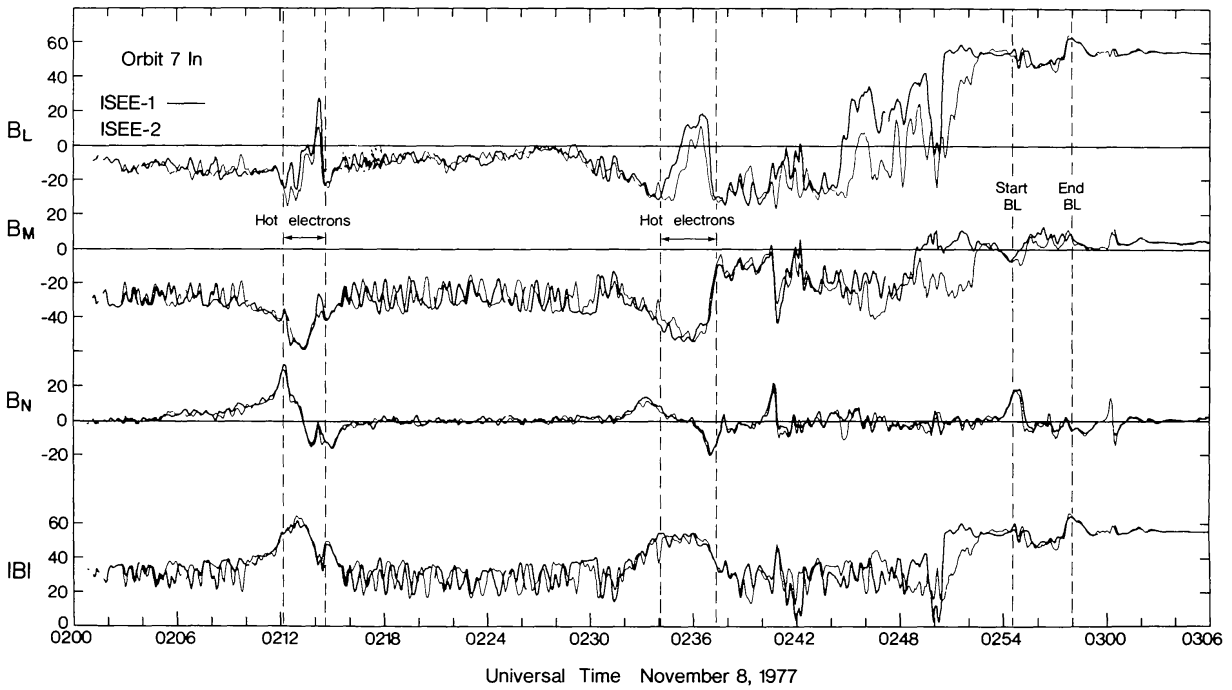

Fig. 9. Medium resolution measurements in boundary normal coordinates across the magnetopause on orbit 7 inbound, November 8, 1977. ISEE-1 measurements are shown with a heavy line, ISEE-2 with a light line. The boundary normal has been taken to be the model normal here. The ISEE spacecraft were at (10.16, −1.77, 5.07)R_e in solar magnetospheric coordinates and separated by 299 km along the normal.

TABLE II
Magnetopause parameters

Time	Nov. 8, 1977 02:45 UT	Nov. 10, 1977 14:50 UT
Orbit	7 inbound	8 inbound
Location $\mathbf{R}_{GSM}$ (R_e)	(10.16, −1.77, 5.07)	(7.09, 0.34, 2.86)
Separation $\mathbf{S}_{GSM}$ (R_e)	(231, −181, 192)	(196, −79, 142)
$\mathbf{B}^{sh}_{GSM}(\gamma)$	(9.2, 18.2, −24.3)	(13.5, 74.0, −48.4)
$\mathbf{B}^{ms}_{GSM}(\gamma)$	(−17.9, −2.0, 52.2)	(−49.5, −2.0, 127.9)
$\sphericalangle \mathbf{B}^{sh}, \mathbf{B}^{ms}$	147.0°	124.8°
${}^{m}\mathbf{n}_{GSM}$	(0.940, −0.108, 0.322)*	(0.962, 0.033, 0.271)
${}^{TD}\mathbf{n}_{GSM}$	(0.945, 0.048, 0.323)	(0.930, 0.066, 0.361)*
$\sphericalangle {}^{n}\mathbf{n}, {}^{TD}\mathbf{n}$	4.1°	5.9°
$\mathbf{S} \cdot \mathbf{n}$	299	228

* Normal used in calculations and plots.

in and out boundary crossing at 02:12 and 02:36 and the field strength reaches magnetospheric levels. However, the B_M and B_N traces exhibit strange behavior at this time. The B_M component becomes much stronger during these events, whereas it is near zero in the magnetosphere. The B_N component has a very peculiar pattern of an increase to large positive values and then a decrease to rather large negative values and then a return to zero. This behavior of B_N is not restricted solely to these apparent magnetopause crossings. There is a similar event at 02:41 and two in the magnetosphere itself: one at 02:57 and one at 03:00. Before examining the magnetopause let us examine these events in detail.

5.1.1. *Flux Transfer Events*

When the magnetic field has a strong component along the magnetopause normal, the immediate conclusion one is tempted to draw is that there is reconnection. However, if reconnection is occurring what is the explanation for the characteristic behavior of B_N and B_M? The first clue is the coherence of the B_N variations at the two spacecraft. The coherence is simply telling us that the variation is associated with a variation in the orientation of the boundary, and the spacecraft are much closer together than the dimensions of the bump in the boundary. The magnetosheath magnetic field has to wrap around that bump in the boundary. The characteristic increase and then decrease through a negative maximum is simply what one would expect if the magnetopause bulged out and this bulge travelled from the nose regions past the spacecraft. We recall that in the magnetosheath B_N is sensitive to oscillations in the $M-N$ plane mainly since the field is mostly along the M-direction whereas in the magnetosphere it is sensitive to oscillations of the boundary orientation in the $L-N$ plane.

The B_L component variation at 02:12 and 02:36 is therefore the signature of a magnetopause entry as expected. The motion of the boundary outward carries the satellites part way into the magnetosphere. We note that B_M increases at these times. In other words the tension in the field lines increases, i.e., the field is

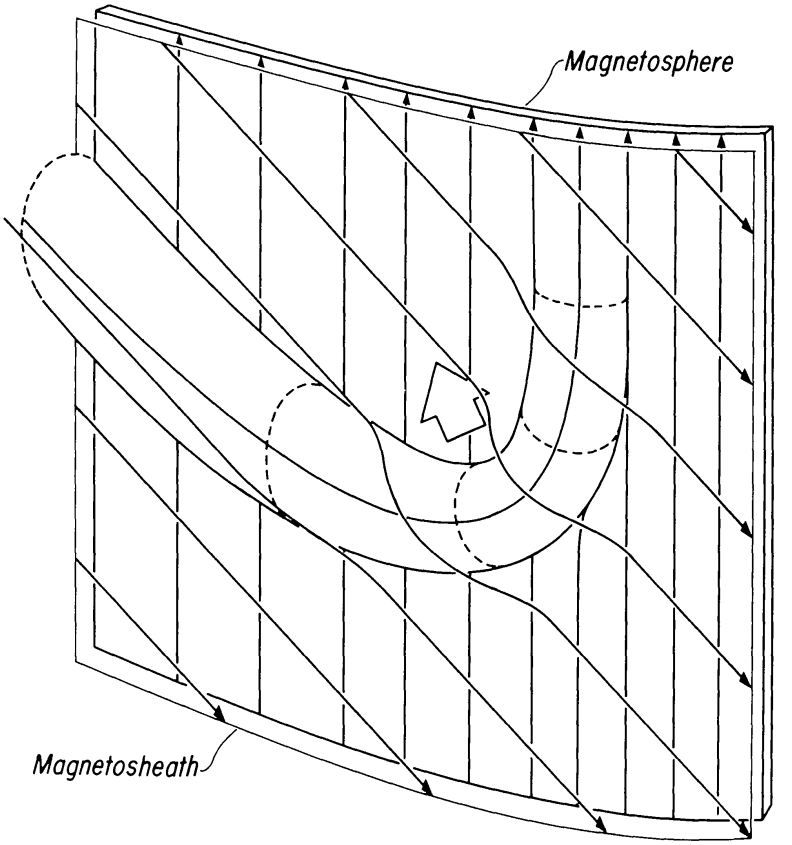

Fig. 10. Qualitative sketch of a flux transfer event. Magnetosheath field lines, slanted arrows, have connected with magnetospheric field lines, vertical arrows, possibly off the lower edge of the figure. As the connected flux tube is carried in the direction of the large arrow by the magnetosheath flow, the stressed field condition at the 'bend' tends to relax, effectively shortening the flux tube and straightening the bend. Magnetosheath field lines not connected to the magnetosphere drape over the connected flux tube and are swept up by its motion relative to the magnetosheath flow.

pulling harder. We note in fact that the B_M component is much stronger in the 'magnetopause' portion of these two events than in the magnetopause crossing at 02:50. Therefore the 'magnetospheric' flux tubes during these times must be bent in the direction of the magnetosheath field.

Our explanation of these events is straightforward. The magnetosphere is undergoing patchy reconnection, and we are seeing flux transfer events. Somewhere upstream of ISEE a magnetospheric flux tube reconnects with the magnetosheath field. Instead of convecting along with the other field lines in the magnetosheath, this reconnected flux tube attempts to shorten itself. This shortening process pulls the magnetospheric field line out of the boundary and twists it out of the vertical direction into the sheath field direction. It also lifts unconnected sheath field lines that overlay the connected lines. Thus we see a B_N increase well before we ever encounter a reconnected tube. These features are depicted schematically in Figure 10.

Patchy reconnection has been postulated before, in connection with high latitude observations (Haerendel *et al.*, 1978). This is the first observation of

patchy reconnection at low latitudes. We do not feel that the reason that patchy reconnection has not been reported before has anything to do with its frequency of occurrence. It is a common feature in magnetic field data. We attribute our successful identification in part to having two satellites and in part to the use of boundary normal coordinates and the use of cartesian components.

Before leaving these events we should remark on the behavior of other instruments during these periods. The LASL/MPI fast plasma instrument measured flowing magnetosheath plasma throughout the 02:12 and 02:36 events. There was a slight drop in the thermal pressure when the field strength increased. We presume that the net effect was to keep the total plasma pressure constant. The direction of the flow also changed characteristically during the event but we have not yet correlated individual flow vectors and field vectors.

The Berkeley/Toulouse electron and proton data show clear 'bursts' of particles at the entries to the 'magnetopause' flux tubes. These bursts have almost identical spectra to the spectra seen later in the outer magnetosphere. In short then, the plasma data say the satellites are in the sheath while the energetic particle data (>2 keV) say the satellites are connected to the magnetosphere.

5.1.2. *The Magnetopause and Boundary Layer*

The magnetopause takes 8 min to cross, because it is oscillating back and forth. These oscillations make the calculation of thickness and velocity very difficult. Fortunately, since the B_N component is fairly steady during this time we can assume that no major changes in boundary orientation occurred and we can use the model normal.

In general the main difference between ISEE-1 and -2 is a time lag with profiles appearing somewhat different because of the variability of the velocity. However, right in the middle of the ISEE-1 crossing there is a feature not duplicated on ISEE-2. At 02:50 the field strength suddenly drops to 2γ. This is not part of the regular boundary structure as defined by the trend in the earlier part of the crossing, or the full crossing on ISEE-2. We will discuss the 'hole' in more detail when we treat the hodograms through the boundary. The only feature in the particle data coincident with the 'hole' that we have found thus far is an increase of close to a factor of 2 in the proton thermal pressure as measured by the LASL/MPI instrument on ISEE-1. Thus the total plasma pressure seems to be conserved through the 'hole' as one would expect.

As indicated on Figure 9 the boundary layer is detached from the magnetopause on this orbit. The boundary layer starts at 02:54:30 and ends at 02:58. We note that the boundary layer begins with a B_N event, which we would interpret as signaling the occurrence of a flux transfer event. The field magnitude is also somewhat depressed within the boundary layer. Further, there is some variation of the field in the M-direction, possibly indicating field aligned currents associated with the boundary layer.

5.2. The microstructure of the boundary

As noted above, the magnetopause crossing on this pass was several minutes in duration, owing to the fact that the boundary oscillated about the mean position of the spacecraft, ISEE-1 making the deeper penetration. This is also apparent in the high resolution data for this crossing, shown in Figure 11a and b, in spacecraft coordinates (approximately GSE); in addition, many high frequency field variations become evident in this figure. ISEE-1 begins to enter the magnetopause at roughly 02:44:30, followed by ISEE-2 at 02:45:00. About 10 s before the ISEE-1 entry, the LASL/MPI instrument indicates that directed bulk flow drops below 40 km s^{-1}, and the same occurs on ISEE-2 at 02:44:30. Flows then reappear at ~02:45:20 on ISEE-1, and persist with variable magnitude until roughly 02:48:15, when a very large bulk flow peak appears. This same feature appears 15 s later on ISEE-2, and reaches approximately 200 km s^{-1} peak flow speed at both spacecraft. In the center of this high speed flow, the fast plasma instrument indicates an enhanced plasma temperature, and the proton energy spectra are peaked at 600–800 eV (see Paschmann *et al.*, 1978). Upon entry into the magnetosphere, at 02:50:30 on ISEE-1 and 02:53:00 on ISEE-2, the

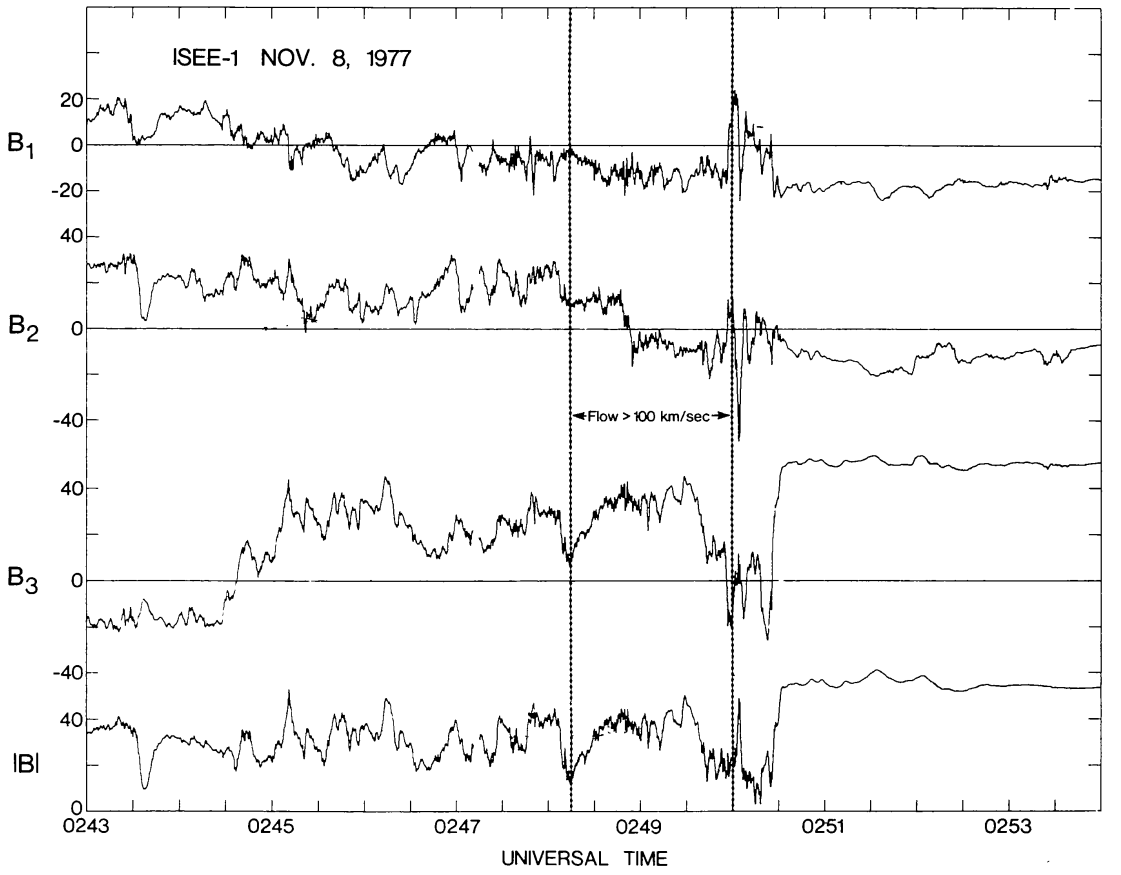

Fig. 11a. High resolution ISEE-1 measurements (16 samples per second) across the magnetopause on November 8, 1977 in spacecraft coordinates. Spacecraft coordinates are within 1° of solar ecliptic coordinates at this time for both satellites.

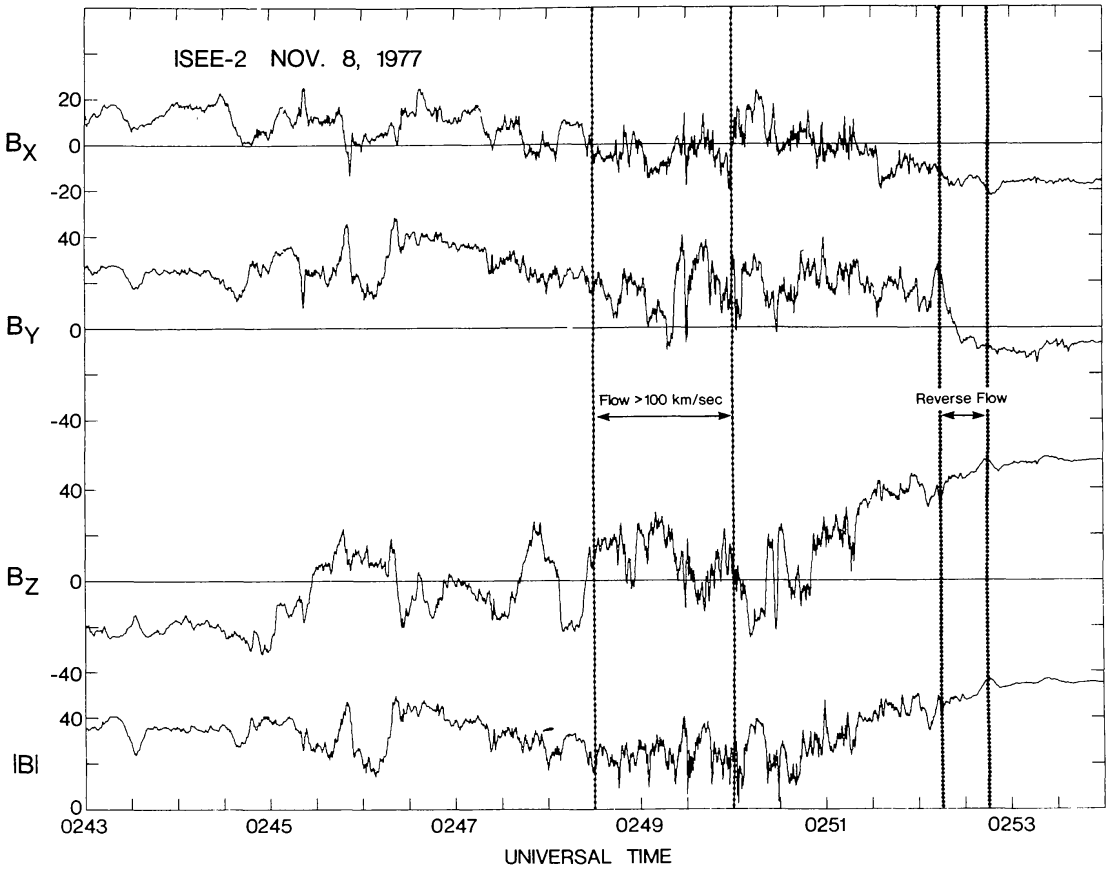

Fig. 11b. High resolution ISEE-2 measurements (16 samples per second) across the magnetopause on November 8, 1977 in spacecraft coordinates.

spacecraft immediately encounter the high temperatures and low densities of outer magnetospheric plasma – no boundary layer is evident until 02:54:30. Also, just before the entry of ISEE-2, a strong (~ 100 km s^{-1}) reverse flow was seen on that spacecraft.

One of the curious aspects of this crossing is the appearance of regions of very low field strength; brief excursions to 3γ or less are not uncommon. As mentioned above, these 'drop-outs' are anticorrelated with proton thermal pressure enhancements, suggesting overall pressure balance. It is noteworthy that such a magnitude drop follows an apparent flux transfer event at 02:50:05 on ISEE-1, which in turn follows the region of high bulk flow speed.

5.3. The Morphology of Flux Transfer Events

The flux transfer events at 02:12 and 02:36 UT cannot be transformed into a coordinate system that reduces the field variations to two dimensions. Therefore we will use the boundary normal coordinate system to display the hodograms of the field variations through the events. Then we will segment one of the crossings for minimum variance analysis. However, only one of these intervals has a well determined normal.

As shown in Figure 12a, the first flux transfer event (FTE) begins in a

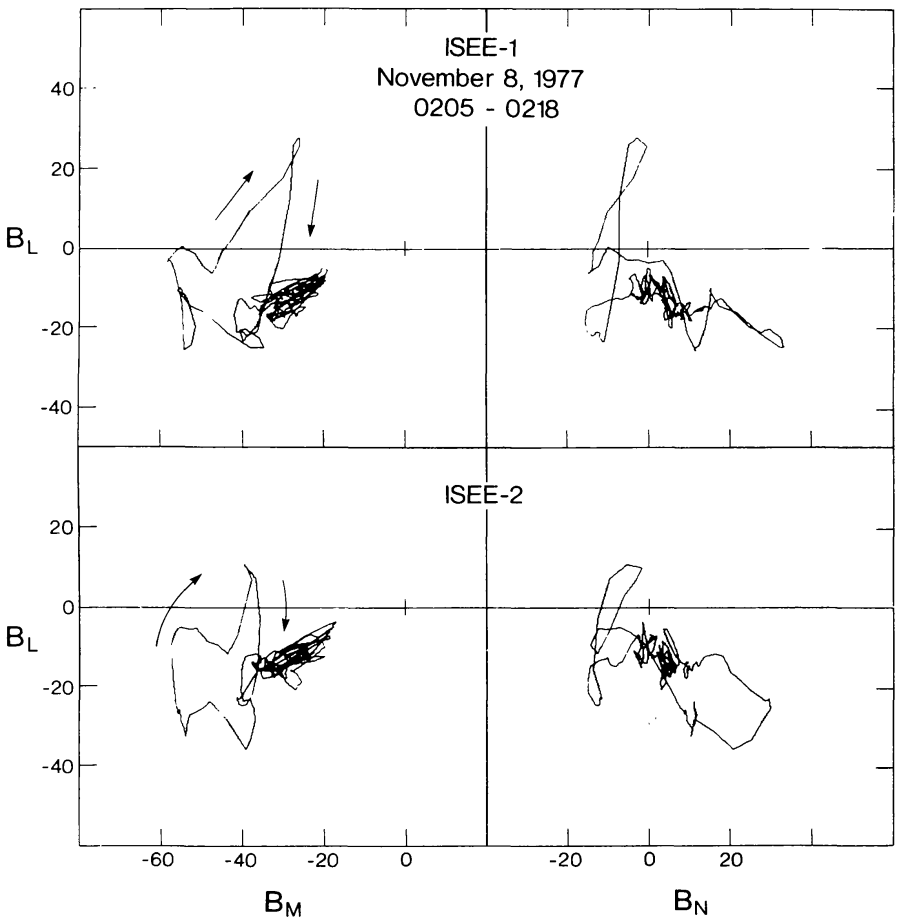

Fig. 12a. Hodogram of medium resolution magnetic field variation on ISEE-1 and -2 during flux transfer event at 02:12 in boundary normal coordinates.

magnetosheath field of roughly $(-10, -25, 0)\gamma$ in the boundary normal coordinates. The B_N component then grows positive, presaging the oncoming 'bump' of the reconnected flux tube, followed by a magnitude enhancement and slight southward turning of the field. Then the B_N component decreases as B_M becomes increasingly negative, corresponding to the stressed magnetosheath field as the 'bump' begins to pass beneath the spacecraft. As the B_M component approaches its extremum, and B_N approaches 10γ, B_L begins to become northward, defining the entry into the flux tube. The excursion reverses itself once as B_M becomes less negative, then continues northward with B_N negative as the spacecraft pass more deeply into the structure. ISEE-1 penetrates the structure more than ISEE-2 as is evident from the higher maximum B_L value. It is during this period that the energetic particles are seen. Exit from the flux tube is then seen with a sudden large decrease in B_L, as B_N remains at negative values, followed by a return to the unperturbed magnetosheath as B_N gradually approaches zero.

The next such occurrence near 02:35, follows the same general sequence of events but with slightly different detail, as shown in Figure 12b. The initial increase in B_N, for example, is much smaller, and entry into the flux tube, as seen

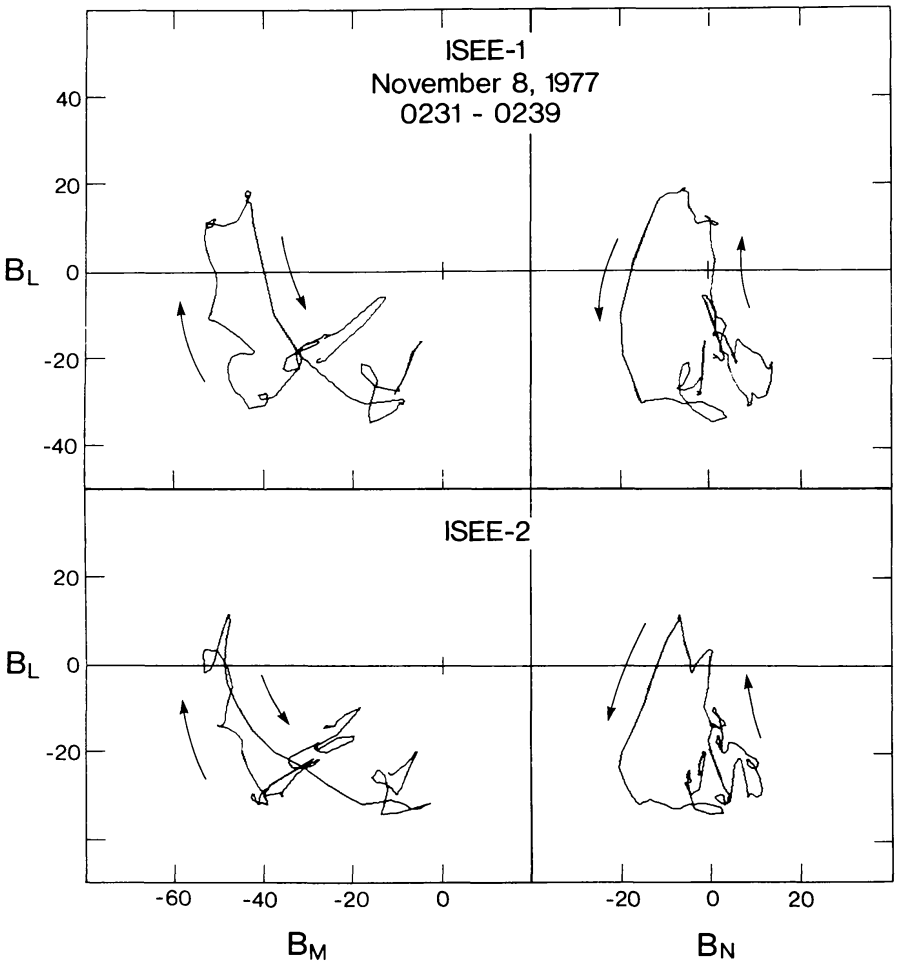

Fig. 12b. Hodogram of medium resolution field variation through flux transfer event at 02:36 UT in boundary normal coordinates.

in the excursion of B_L, occurs from a field somewhat more strongly southward than on the previous occasion. In addition, the final configuration of the magnetosheath field is different from the initial configuration. It should be mentioned that the plasma bulk flow direction between 02:33 and 02:34 is much more nearly antisunward than the unperturbed magnetosheath flow, in accord with the notion that the positive B_N component at this time reflects magnetosheath flow about an obstacle upstream of the spacecraft. Likewise, the flow direction between 02:37:30 and 02:38:00 from the LASL/MPI instrument is more nearly dawnward than unperturbed magnetosheath flow, as would be expected if an obstacle downstream on the boundary were deflecting the magnetosheath around it; this is also suggested by the negative value of B_N at this time. For both events, the final exit through the current layer defining the magnetosheath/flux tube interface at the upstream side is more discrete than initial entry through the downstream interface.

To contrast the behavior of the magnetopause crossing with the two FTE's we show in Figure 12c the magnetopause crossing near 02:50 in the same type of

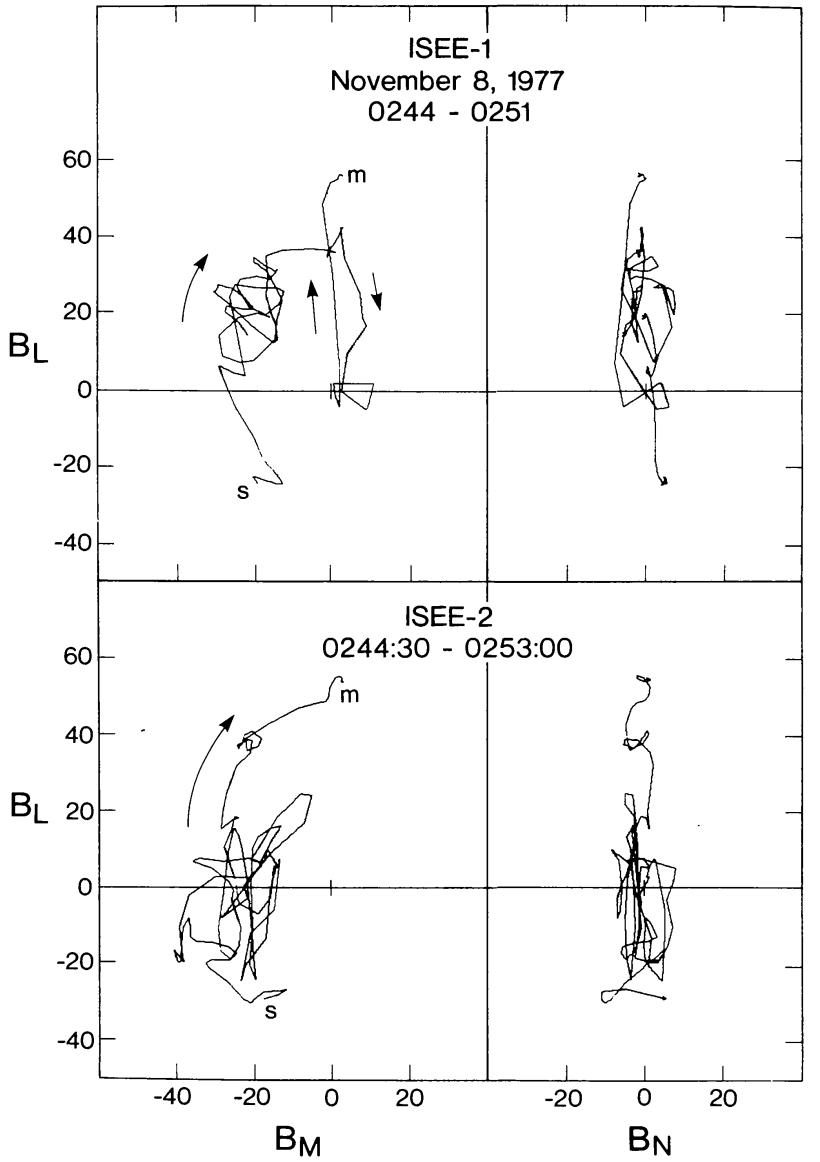

Fig. 12c. Hodogram of medium resolution field variation through magnetopause at 02:50 UT in boundary normal coordinates.

display. The initial rotation from magnetosheath to magnetosphere is interrupted by the sudden change in motion of the boundary, which oscillates about the spacecraft. ISEE-1, having penetrated deeper into the magnetopause before the motion change, shows excursions about a different average phase of the rotation than ISEE-2. ISEE-1 then passes into a region of very small field strength, before finally attaining the magnetospheric configuration. ISEE-2, meanwhile, shows no hint of the low field structure. Thus, the scale size of this 'hole' appears to be less than the separation of the spacecraft.

To see if some portions of an FTE might be reduced to a two-dimensional variation we have performed an eigenvalue analysis on the entry and exit from the flux tube. These analyses are shown in Figure 13. The eigenvalues for the entry

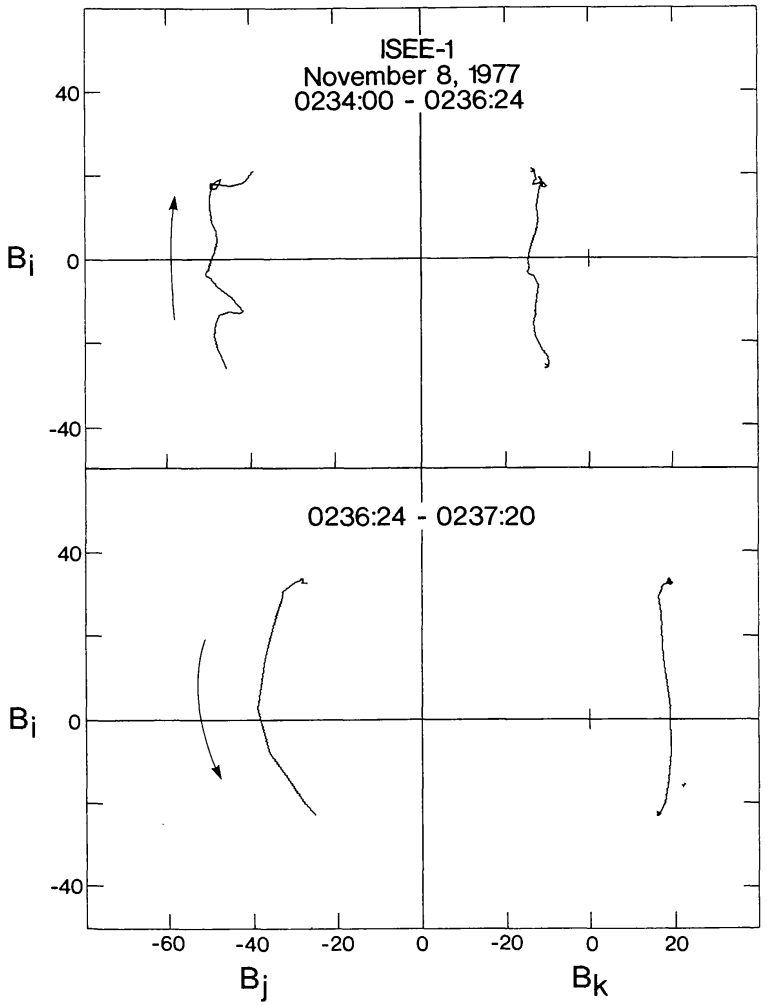

Fig. 13. Hodogram of medium resolution field variation through entry and exit of flux transfer event in principal axis system.

are $(233, 8, 2)\gamma^2$ with eigenvectors associated with the maximum eigenvalue of (0.976, −0.134, −0.174) and with the minimum eigenvalue of (0.205, 0.268, 0.941) in boundary normal coordinates. This direction is 20° from the undisturbed normal. It is also 12° up out of the $M-N$ plane and tilted back 16° from the $L-N$ plane, with a probable error of 14°. These angles are quite consistent with the picture of a flux tube being lifted up and back by reconnection with the magnetosheath field.

A similar analysis for the exit yields eigenvalues of $(451, 16, 1)\gamma^2$, and a minimum variance eigenvector of (−0.435, −0.692, 0.576) in boundary normal coordinates. This vector is 55° from the undisturbed normal, tilted down 26° from the $M-N$ plane, and 44° forward (sunward) from the $L-N$ plane. The probable error in direction of this eigenvector is only 7°, so that the orientation is consistent with passage through the trailing edge of the flux tube. As can be seen in Figure 13, there is a well-defined component of $18\pm4\gamma$ normal to the flux tube/magnetosheath interface, suggesting that reconnection may still be occurring at this point.

To approximate the amount of flux eroded during a flux transfer event we must estimate the cross-section of the reconnected flux tube and the flux passing through this cross-section. The duration of the flux tube crossing gives us an estimate of one dimension assuming it is convecting by with the speed of the plasma. This dimension is $4R_e$ for both FTE's, the longer duration of the second FTE being due to a slower flow velocity. Assuming that the orthogonal dimension is similar since the normal appears to have been rotated by about 45° during the passage of the flux tube, and we obtain a flux of 3×10^{15} Mx for the first FTE and 2×10^{15} for the second. At a rate of 2–3 per hour, these events represent an erosion rate of about 2×10^{12} Mx s^{-1}. This rate is similar to that found by Aubry *et al.* (1970) when the magnetosheath field had a southward component of about 30γ, compared with the approximately 10γ southward field before the flux transfer events at 02:12 and 02:36 UT. Thus, these FTE's are not merely curiosities, but in fact large enough to be significant if not dominant in the erosion of the dayside magnetopause.

6. Southward Magnetosheath Field, Orbit 8 In

On orbit 8 inbound the magnetopause was encountered far inward of its usual position at (7.09, 0.34, 2.86)R_e in solar magnetospheric coordinates. This unusual location is manifested in Figure 14 by the large field values both in the magnetosheath and in the magnetosphere. The angle between the model normal and the normal obtained assuming that the boundary was a tangential discontinuity during the quiet intervals on this day (see Table II) was 5.9° while this is a moderately small difference, the data are better ordered by the tangential discontinuity normal and we will use this normal for our discussion and data display. The separation along the normal was 228 km.

6.1. Macrostructure of the Boundary

The medium resolution data in magnetopause normal coordinates in Figure 14 show there are three main magnetopause crossings. The B_N component shows that these crossings are accompanied by many (at least 8) large deviations of the boundary normal. These have all the characteristics of the flux transfer events of the orbit 7 inbound crossing except that the duration of the events is much shorter. The events show a positive enhancement of B_N followed by a negative depression. Variance analysis shows they are three dimensional. They do not have a single principal plane of field change. Further, they contain hot magnetospheric-like electrons (and protons too) when they occur in the magnetosheath. We will not discuss the presence of hot particles at B_N fluctuations in the magnetopause or magnetosphere, because we expect these particles in these regions at all times. Perhaps, the most important new facet of this series of crossings is the fact that the flux transfer events are occurring almost continually. They are in fact

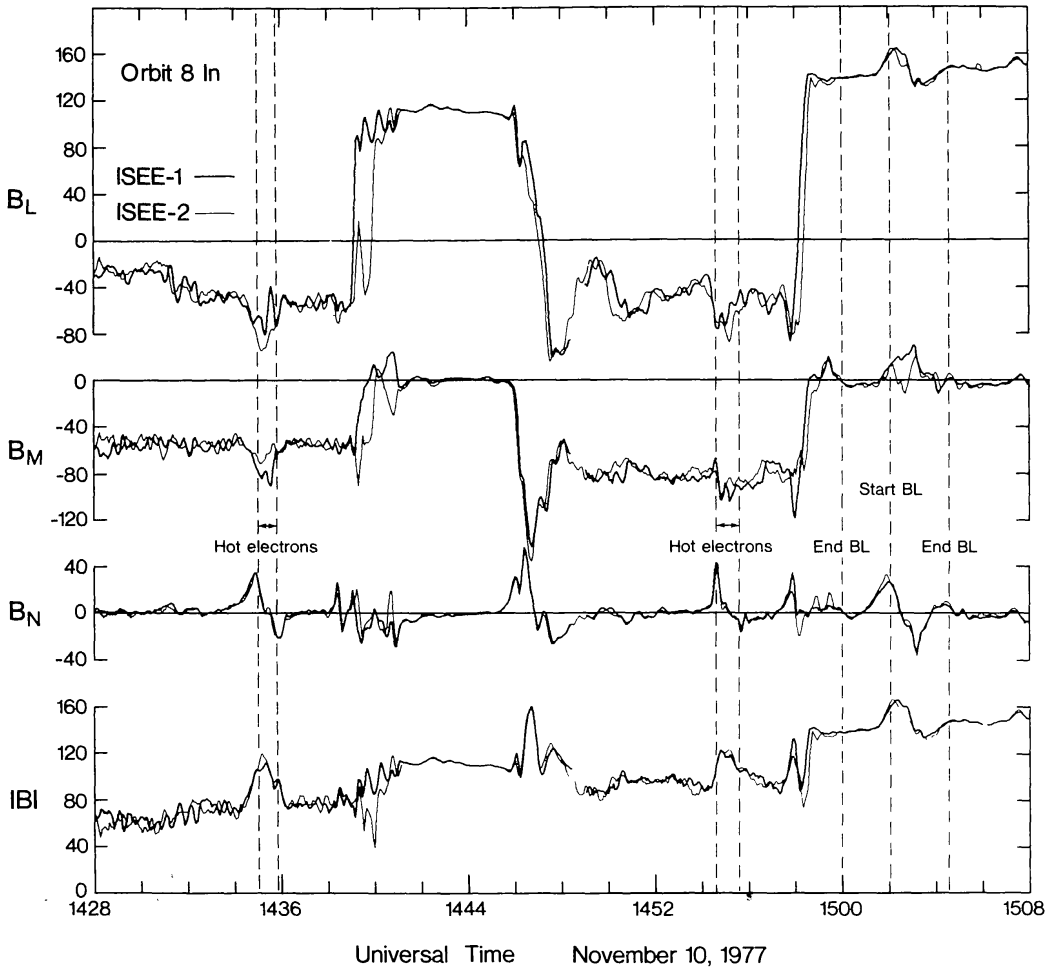

Fig. 14. Medium resolution measurements in boundary normal coordinates across magnetopause on orbit 8 inbound, November 10, 1977. ISEE-1 measurements are shown with a heavy line; ISEE-2 with a light line. The boundary normal has been taken to be the tangential discontinuity normal here. The ISEE spacecraft were at (7.09, 0.34, 2.86)R_e in solar magnetospheric coordinates and were separated by 228 km along the boundary normal.

occurring as the ISEE spacecraft cross the magnetopause on all three occasions. We note that within the magnetosphere the boundary layer ceases on both spacecraft at 15:00 UT and reappears at 15:02, only to cease again at 15:04:30. The behavior suggests that the appearance may be temporal rather than spatial. We also note that the B_M fluctuations in the boundary layer suggest the presence of field-aligned currents.

6.2. Microstructure of the Boundary

The magnetopause crossings observed on this day are all complicated by the presence of flux transfer events in or near the boundary. The first crossing, near 14:40, is shown in high resolution in Figure 15. ISEE-1, 228 km inward along the normal from ISEE-2, appears to enter the magnetopause at 14:39, as evidenced by the strong northward excursion of the B_L component. The variations in the sign of B_N, as well as the enhancement in B_M, also suggest a flux transfer event.

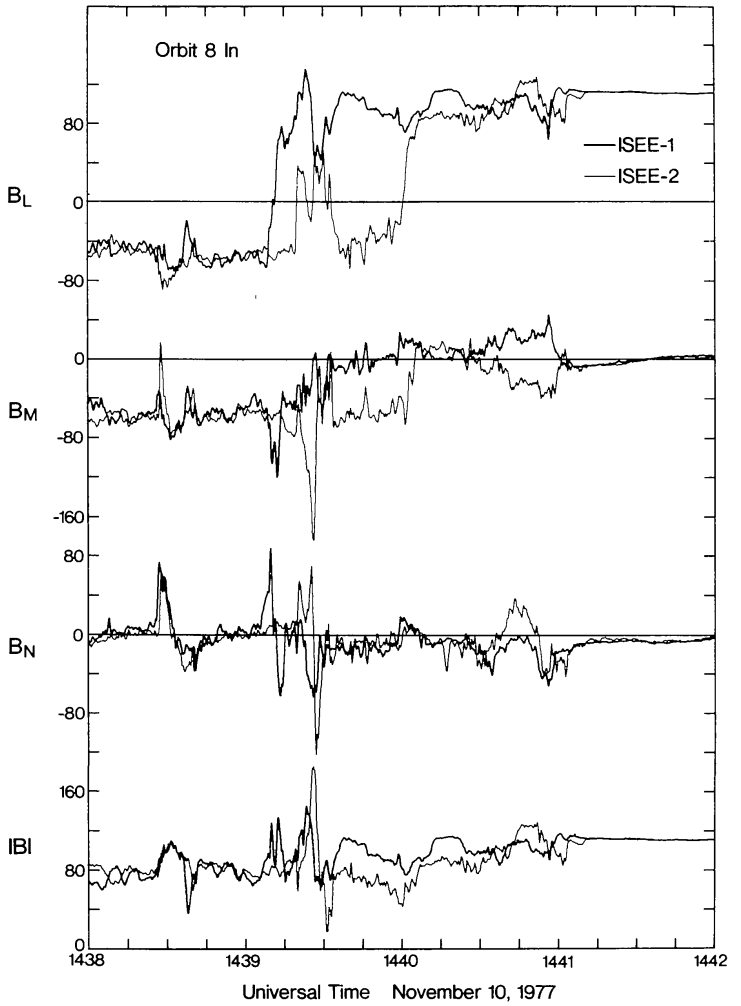

Fig. 15. High resolution measurements (four samples per second) across the first magnetopause crossing on November 10, 1977 expressed in boundary normal coordinates.

At 14:40, however, the field configuration is nearly magnetospheric, though considerable noise is present. Finally, entry into the quiet magnetosphere takes place at 14:41. Meanwhile, ISEE-2 also enters the flux tube near 14:39:20, but the field is more nearly horizontal and of higher magnitude than at the ISEE-1 entry. Then ISEE-2 reenters the magnetosheath soon after 14:39:30, while ISEE-1 is in a magnetospheric configuration; thus, the current layer thickness must be less than the total spacecraft separation distance, 255 km. Entry into the true magnetosphere shortly after 14:41 on ISEE-2 is accompanied by the sudden drop in density and increase in temperature which signals the disappearance of magnetosheath plasma. High speed ($>100\,\mathrm{km\,s^{-1}}$) flows are seen at 14:39:30 and 14:40:30 on ISEE-2. The first has a dawnward horizontal component, and coincides with the spacecraft's flight through the flux tube while the second flow has a horizontal component directed inward from the boundary, and occurs after ISEE-2's entry into magnetosphere-like field. The plasma and particle instruments on ISEE-1 were turned off at this time.

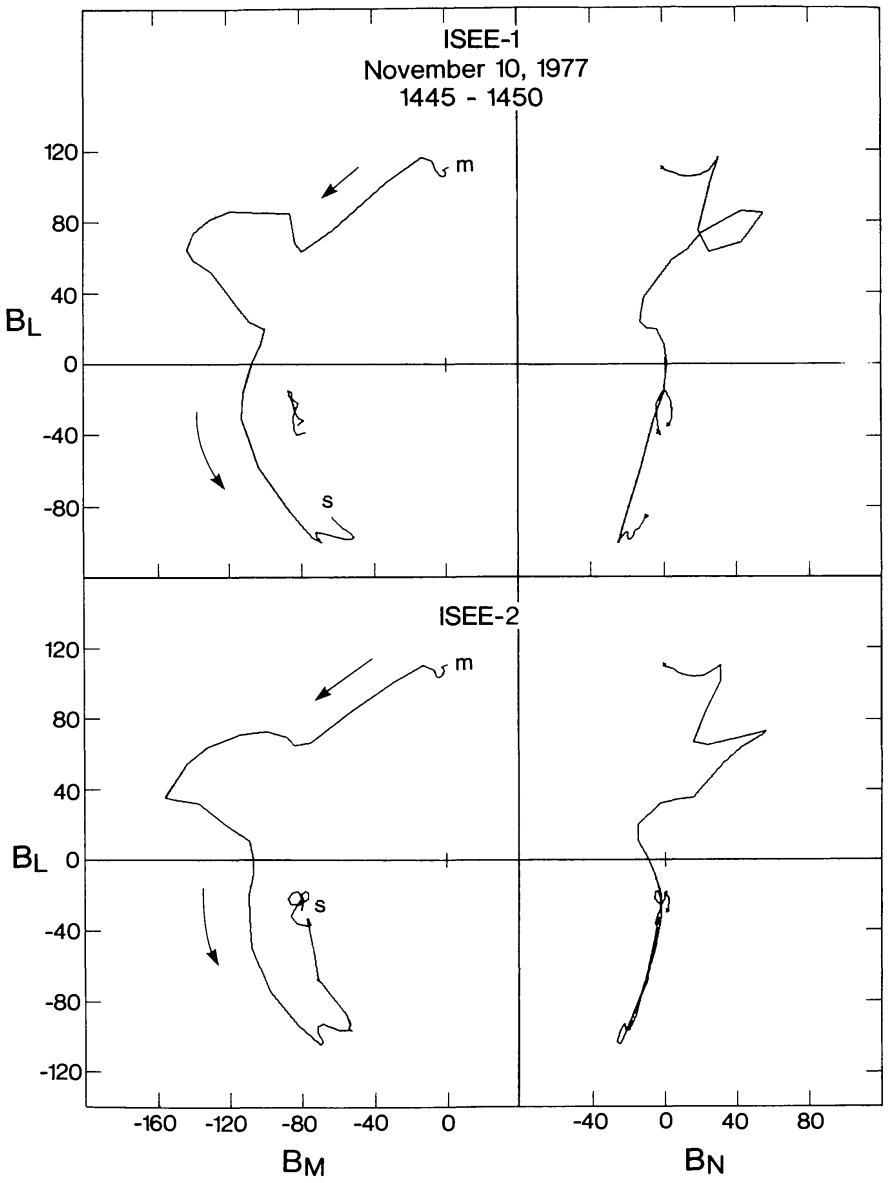

Fig. 16. Hodogram of medium resolution field measurements through the second magnetopause crossing on November 10, 1977 in boundary normal coordinates.

The second crossing of the magnetopause at 14:47 includes another FTE. Here again, the transition from hot, tenuous magnetospheric plasma to magnetosheath plasma occurs before any appreciable field direction change, at 14:46:10. Hodograms of medium resolution data in boundary normal coordinates appear in Figure 16. First, the B_N component increases, followed by the initial phase of the field rotation. Abruptly, the magnitude increases, as does B_N, and the rotation continues. B_N then becomes slightly negative as B_M returns from its excursion. The B_L component continues to turn southward, and a mild enhancement of B_M occurs again, followed by rotation to a southward extremum before returning to unperturbed magnetosheath. A bulk flow maximum of ~ 150 km s^{-1} occurs at the

first B_M enhancement, and speeds of $\sim 100\ \mathrm{km\ s^{-1}}$ prevail throughout the rest of the structure.

Another FTE is encountered just before the third and final magnetopause crossing at about 14:58:30. The plasma flow speed seen at the time of this event is $\sim 45\ \mathrm{km\ s^{-1}}$, which increases to $\sim 100\ \mathrm{km\ s^{-1}}$ at the magnetopause. This entry, unlike the previous two, is accompanied by the appearance of a boundary layer.

6.3. Flux transfer events

Because of the many flux transfer events on this day, it is of interest to determine whether a correspondingly large amount of flux is being transported from the dayside. The first event in which significant penetration of the flux tube occurs is also the initial 'magnetopause' crossing. Using, as before, the LASL/MPI bulk flow speed, the peak B value and the duration of the event, an approximate total area of $4\times10^7\ \mathrm{km^2}$ results, giving a net flux of 6×10^{14} Mx. The second useable event is during the second crossing, with a duration of about 36 s, giving an area of $\sim 2\times10^7\ \mathrm{km^2}$ (linear dimension of about $0.7R_e$), yielding a transported flux of about 2.2×10^{14} Mx. The last useful event, just before the third crossing, gives a flux of 3×10^{14} Mx. The flux transferred per event here is smaller than on November 8, but if in the period of a half hour eight intermediate (4×10^{14} Mx) events take place, the rate of the flux removal is about $2\times10^{12}\ \mathrm{Mx\ s^{-1}}$, a number very similar to that calculated for the previous orbit in Section 5.3. We note that these numbers should be lower limits to the true rate since depending on satellite location events could be missed by ISEE and further reconnection could take place after the FTE has passed by ISEE.

6.4. Velocity and thickness

Since the first two magnetopause crossings are complicated by FTE's, the direction of motion of the boundary is poorly determined. The third crossing, however, has no such problem, and the thickness calculated by stepping through the boundary turns out to be between 680 and 912 km. Speeds range from 11.5 to $20.9\ \mathrm{km\ s^{-1}}$ on this crossing. As discussed in Section 6.2, the current sheet thickness for the crossing near 14:40 must be less than 255 km, but the velocity of the structure is nearly impossible to determine given its three dimensional nature and temporal evolution. On the other hand, the structure seen on the second crossing at 14:47 is apparently much larger than the separation of the two spacecraft, since at any time the two spacecraft see fields which are but slightly different (see Figure 14). Such apparent near simultaneity can be caused by motion largely transverse to the spacecraft separation vector, such as could occur when a fluxtube containing both spacecraft becomes reconnected and is pulled tangential to the boundary, leaving the spacecraft to pass almost simultaneously into the magnetosheath. Thus, on this day, boundary thickness from less than 255 km to 912 km and possibly larger may have occurred.

7. Conclusions

The studies presented here represent only the beginnings of our investigation of the magnetopause. In particular we plan to undertake a survey of the behavior of the magnetopause over a wider range of longitudes including both morning and afternoon local times and under a wider range of magnetosheath field directions. Until such a survey is performed we will not be able to tell how typical are the signatures observed here (near local noon) and exactly where the flux transfer events are initiated. With the present set of data we cannot tell whether the flux transfer events begin at the polar cusp (the south polar cusp for the events we saw) or in the equatorial regions. A study of where they are observed as a function of B_M (or B_Y GSM) should be able to resolve this question.

It is clear from the data that the structure of the magnetopause is complex. This complexity arises in part from the impulsive and three-dimensional nature of the flux transfer event. The boundary is often not time stationary and its normal varies in direction during a crossing. Even when the magnetosheath field is northward and flux transfer events are not seen, the motion of the boundary is irregular, changing markedly in the length of time it takes to cross a boundary, thus complicating our attempts to place dimensions on the thickness of the magnetopause. On the one boundary crossing studied under northward magnetosheath conditions, the major current layer was over 1000 km thick but the total boundary thickness was probably over 2000 km. A further interesting aspect was that the field strength in the magnetopause itself was greater than in either the magnetosheath or the magnetosphere.

When the interplanetary field was southward, the magnetopause appeared to be thinner, usually in the range 500–1000 km thick. However, this determination is complicated by the irregularity in motion, the changes in boundary orientation, and the time variability of the structure. In particular the occasional occurrence of drop-outs in the field strength, to very low values during crossings on one of the spacecraft and not on the other is very intriguing.

Flux transfer events naturally lead to oscillations in the position of the magnetopause as they propagate from the subsolar regions down the flanks of the magnetosphere much in the same way the Kelvin-Helmholtz instability should lead to boundary oscillations. Furthermore, flux transfer events probably, although we have not proven this, occur more readily at high solar wind velocities, just as the Kelvin-Helmholtz instability should be more effective at high solar wind velocities (Boller and Stolov, 1970; Boller and Stolov, 1973). The difference between the two mechanisms is that the Kelvin-Helmholtz mechanism is independent of whether the magnetosheath field is northward or southward. Until investigations of the dependence of boundary motions and pulsation amplitudes on the direction of the north-south component of the interplanetary field are undertaken we must reserve judgment on the efficacy of the Kelvin-Helmholtz mechanism in producing magnetic pulsations in the outer magnetosphere.

A complete study of the magnetopause requires a detailed examination of the joint plasma and field behavior including the three-dimensional flows present. Such work has just begun. However, the excellence of the ISEE data, together with the spirit of cooperation shown by the various experiment groups promises returns limited only by the resources available to support such studies.

Acknowledgements

We are grateful for the spirit of free data exchange and cooperation exhibited by the various investigator groups on the ISEE spacecraft. In particular in this paper we benefited much from the data from the LASL/MPI fast plasma instrument and the Berkeley/Toulouse energetic particle experiment. Discussions of these data with G. Paschmann (LASL/MPI), G. Parks, K. Anderson, and R. Lin (Berkeley/Toulouse) were most welcome. We are grateful to K. Anderson for sponsoring two of the workshops at which much of this exchange took place.

We should mention some of the many people who contributed to the success of the spacecraft and helped maintain a magnetically clean vehicle so that these studies could be performed: J. Madden and M. Davis of GSFC and D. Eaton and R. Gruen of ESTEC. The instrument itself was ably built, tested and calibrated by B. Plitt and his staff of Westinghouse and R. Snare, F. George, and J. Means of UCLA. We are also indebted to R. Walker, H. Singer, and S. Kaye for assisting us with the initial data processing. The flipper design was kindly provided by C. P. Sonett.

This research was conducted for the National Aeronautics and Space Administration under contract NAS 5-20064.

References

Arnoldy, R. L.: 1971, 'Signature in the Interplanetary Medium for Substorms', *J. Geophys. Res.* **76,** 5189.

Aubry, M. P., Russell, C. T., and Kivelson, M. G.: 1970, 'Inward Motion of the Magnetopause Before a Substorm', *J. Geophys. Res.* **75,** 7018.

Aubry, M. P., Kivelson, M. G., and Russell, C. T.: 1971, 'Motion and Structure of the Magnetopause', *J. Geophys. Res.* **76,** 1673.

Binsack, J. H.: 1968, 'Shock and Magnetopause Boundary Observations with IMP-2', in R. L. Carovillano, J. F. McClay, and H. R. Radoski (eds.), *Physics of the Magnetosphere*, D. Reidel Publ. Co., Dordrecht, p. 605.

Boller, B. R. and Stolov, H. L.: 1970, 'Kelvin-Helmholtz Instability and the Semi-Annual Variation of Geomagnetic Activity', *J. Geophys. Res.* **75,** 6073.

Boller, B. R. and Stolov, H. L.: 1973, 'Explorer-18 Study of the Stability of the Magnetopause Using a Kelvin-Helmholtz Instability Criterion', *J. Geophys. Res.* **78,** 8078.

Bridge, H., Egidi, A., Lazarus, A., Lyon, E., and Jacobson, L: 1965, 'Preliminary Results of Plasma Measurements on IMP-A', *Space Research* **V,** North-Holland Publ. Co., Amsterdam, p. 969.

Burton, R. K., McPherron, R. C., and Russell, C. T.: 1975, 'An Interplanetary Relationship Between Interplanetary Conditions and Dst', *J. Geophys. Res.* **80,** 4204.

Cahill, L. J. and Amazeen, P. G.: 1963, 'The Boundary of the Geomagnetic Field', *J. Geophys. Res.* **68,** 1835.

Cahill, L. J. and Patel, V. L.: 1967, 'The Boundary of the Geomagnetic Field, August to November, 1961', *Planetary Space Sci.* **15,** 997.

Cummings, W. D. and Coleman, P. J., Jr.: 1968, 'Magnetic Fields in the Magnetopause and Vicinity at Synchronous Altitude', *J. Geophys. Res.* **73,** 5699.

Fairfield, D. H.: 1971, 'Average and Unusual Locations of the Earth's Magnetopause and Bow Shock', *J. Geophys. Res.* **76,** 6700.

Feldstein, Y. I.: 1970, 'Auroras and Associated Phenomena', in E. R. Dyer (ed.), *Solar Terrestrial Physics,* Part III, D. Reidel Publ. Co., Dordrecht, p. 152.

Frank, L. A. and Van Allen, J. A.: 1964, 'Intensity of Electrons in the Earth's Inner Radiation Zone', *J. Geophys. Res.* **69,** 4923.

Freeman, J. W., Jr.: 1964, 'Detection of an Intense Flux of Low-Energy Protons or Ions Trapped in the Inner Radiation Zone', *J. Geophys. Res.* **69,** 1691.

Gosling, J. T., Asbridge, J. R., Bame, S. J., and Strong, I. B.: 1967, 'Vela-2 Measurements of the Magnetopause and Bow Shock Positions', *J. Geophys. Res.* **72,** 101.

Haerendel, G., Paschmann, G., Sckopke, N., Rosenbauer, H., and Hedgecock, P. C.: 1978, 'The Frontside Boundary Layer of the Magnetosphere and the Problem of Reconnection', *J. Geophys. Res.* **83,** 3195.

Heppner, J. P., Sugiura, M., Skillman, T. L., Ledley, B. G., and Campbell, M.: 1967, 'OGO-A Magnetic Field Observations', *J. Geophys. Res.* **72,** 5417.

Holzer, R. E. and Slavin, J. A.: 1978, 'Magnetic Flux Transfer Associated with Expansions and Contractions of the Dayside Magnetosphere', *J. Geophys. Res.* **83,** 3831.

Holzer, R. E., McLeod, M. G., and Smith, E. J.: 1966, 'Preliminary Results from the OGO-1 Search Coil Magnetometer: Boundary Positions and Magnetic Noise Spectra', *J. Geophys. Res.* **71,** 1481.

Kaufmann, R. L. and Konradi, A.: 1969, 'Explorer-12 Magnetopause Observations: Large-Scale Non-Uniform Motion', *J. Geophys. Res.* **74,** 3609.

Kaufmann, R. L. and Konradi, A.: 1973, 'Speed and Thickness of the Magnetopause', *J. Geophys. Res.* **78,** 6549.

Ledley, B. G.: 1971, 'Magnetopause Attitudes During OGO-5 Crossings', *J. Geophys. Res.* **76,** 6736.

Meng, G.-I.: 1970, 'Variation of the Magnetopause Position with Substorm Activity', *J. Geophys. Res.* **75,** 3252.

Mozer, F. S., Torbert, R. B., Fahleson, U. V., Fälthammar, C.-G., Gonfalone, A., Pedersen, A., and Russell, C. T.: 1978, *Geophys. Res. Letters,* submitted.

Ness, N. F., Sceorce, C. S., and Seek: 1964, 'Initial Results of the IMP-1 Magnetic Field Experiment', *J. Geophys. Res.* **69,** 3531.

Ness, N. F.: 1967, in J. W. King and W. S. Newman (eds.), *Solar Terrestrial Physics,* Academic Press, London, p. 57.

Neugebauer, M., Russell, C. T., and Smith, E. J.: 1974, 'Observations of the Internal Structure of the Magnetopause', *J. Geophys. Res.* **79,** 499.

Ogilvie, K. W., Scudder, J. D., and Sugiura, M.: 1971, 'Magnetic Field and Electron Observations Near the Dawn Magnetopause', *J. Geophys. Res.* **76,** 3574.

Paschmann, G., Sckopke, N., Haerendel, G., Papamastorakis, J., Bame, S. J., Asbridge, J. R., Gosling, J. T., Hones, E. W., Jr., and Tech, E. R.: 1978, 'ISEE Plasma Observations Near the Subsolar Magnetopause', *Space Sci. Rev.* **22,** 717.

Patel, V. L. and Dessler, A. J.: 1966, 'Geomagnetic Activity and Size of Magnetospheric Cavity', *J. Geophys. Res.* **71,** 1940.

Russell, C. T.: 1978, 'The ISEE-1 and -2 Fluxgate Magnetometers', *IEEE Trans. Geosci. Electr.* **GE-16,** 239.

Russell, C. T. and Greenstadt, E. W.: 1979, 'Initial ISEE Magnetometer Results: Shock Observations,' *Space Sci. Rev.* **23,** in press.

Russell, C. T. and McPherron, R. L.: 1973, 'The Magnetotail and Substorms', *Space Sci. Rev.* **15,** 205.

Russell, C. T., Neugebauer, M., and Kivelson, M. G.: 1974, 'OGO-5 Observations of the Magnetopause', in D. E. Page (ed.), *Correlated Interplanetary and Magnetospheric Observations,* D. Reidel Publ. Co., Dordrecht, p. 139.

Sonnerup, B. U. O.: 1971, 'Magnetopause Structure During the Magnetic Storm of September 24, 1961', *J. Geophys. Res.* **76,** 6717.

Sonnerup, B. U. O. and Cahill, L. J., Jr.: 1967, 'Magnetopause Structure and Attitude from Explorer-12 Observations', *J. Geophys. Res.* **72,** 171.

Sonnerup, B. U. O. and Cahill, L. J., Jr.: 1968, 'Explorer-12 Observations of the Magnetopause Current Layer', *J. Geophys. Res.* **73,** 1757.

Sonnerup, B. U. O. and Ledley, B. G.: 1974, 'Magnetopause Rotational Forms', *J. Geophys. Res.* **79,** 4309.

Sonnerup, B. U. O. and Ledley, B. G.: 1978, 'OGO-5 Magnetopause Structure and Classical Reconnection', *J. Geophys. Res.*, submitted.

Wolfe, J. H., Silva, R. W., and Meyers, M. A.: 1966, 'Observations of the Solar Wind During the Flight of IMP-1', *J. Geophys. Res.* **71,** 1319.